View Article Online
View Journal

Dalton Transactions

An international journal of inorganic chemistry

Accepted Manuscript

This article can be cited before page numbers have been issued, to do this please use: C. Bisio, J. Brendle, S. Cahen, Y. Feng, S. Hwang, K. Melanova, M. Nocchetti, D. O'Hare, P. Rabu and F. Leroux, *Dalton Trans.*, 2024, DOI: 10.1039/D4DT00755G.

ROYAL SOCIETY OF CHEMISTRY

rsc.li/dalton

Data availability statement

View Article Online
DOI: 10.1039/D4DT00755G

Manuscript Ms. Ref. No.: DT-PER-03-2024-000755 entitled "*Recent Advances and Perspectives for Intercalation Compounds Part 1: Design and applications in the field of energy* ", authored by *Chiara Bisio, Jocelyne Brendlè, Sébastien Cahen, Yongjun Feng, Seong-Ju Hwang, Morena Nocchetti, Dermot O'Hare, Pierre Rabu, Klara Melanova, Fabrice Leroux*.

No primary research results, software or code have been included and no new data were generated or analysed as part of this review.

View Article Online
DOI: 10.1039/D4DT00755G

Perspectives

fReceived 00th January[i] 20xx,Accepted 00th January 20x

DOI: 10.1039/x0xx00000x

Recent Advances and Perspectives for Intercalation Layered Compounds.

Part 1: Design and applications in the field of energy

Chiara Bisio,[a,b*] Jocelyne Brendlé,[c*] Sébastien Cahen,[d] Yongjun Feng,[e] Song-Ju Hwang,[f] Klara Melanova,[g] Morena Nocchetti,[h*] Dermot O'Hare,[i] Pierre Rabu,[j] Fabrice Leroux[k*]

After a general overview of the overworld financial support for chemistry devoted to materials science and more specifically to intercalation layered compounds (ILCs), the strategies to synthesize such host structure and subsequent guest-host hybrid assembly are exemplified on the basis of some families of materials including pillared clays (PILC), porous clay heterostructure (PCH), Zirconium phosphate (ZrP), layered double hydroxide (LDH), graphite intercalation compounds (GIC), graphene-based, MXenes… Additionally a non-exhaustive survey on their possible application in the field of energy through electrochemical storage mostly as electrode materials but also as electrolyte additives is presented including lithium technologies based on lithium ion batterie (LIB) and also «beyond LiBs» with a focus on the possible alternatives such XIB (X = Na (NIB), K (KIB), Al (AIB), Zn (ZIB), Cl (CIB), reversible Mg batteries (RMB), Dual-ion batteries (DIB), Zn-air, Zn-sulphur… and supercapacitors as well as their relevance in other fields regarding (opto)electronics. This selective panorama should help to better understand the reason why ILCs are expected to meet the challenge of tomorrow as electrode materials.

Introduction

Today even more than before science is questioned to improve our daily lives and more specifically the science of materials must respond to new challenges concerning the major human issues including breakthrough solutions such as health, energy and mobility, agriculture and environment and so on, this by respectful approaches of sustainable development and if possible, of the circular economy. These ever-increasing levels of requirement are causing certain technologies to be rethought, considering the carbon footprint, the reduction of fossil fuels, the rarefaction of the elements and their balance from the mine to their end of life, the so-called life cycle assessment combined with their sustainable development during their period of use. As scientists, we must take these criteria into consideration because we are creating the materials of tomorrow.

There is a real need for fundamental research to feed its successes into today's technologies by crossing the famous Technology Readiness Levels (TRLs) as quickly as possible from proof of concept to prototype manufacturing. Because of their reactivity, layered materials and more generally intercalation compounds are of great interest for many fields such as catalysis, photo-physical processes, electronics, energy, drug delivery, biomaterials, coatings, composites as polymer fillers, and water remediation. Funding agencies

[a.] *Dipartimento di Scienze e Innovazione Tecnologica, Università del Piemonte Orientale, Viale Teresa Michel 11, 15121 Alessandria (AL), Italy; chiara.bisio@uniupo.it
[b.] *CNR-SCITEC Istituto di Scienze e Tecnologie Chimiche "Giulio Natta", Via C. Golgi 19, 20133 Milano (MI), Italy.
[c.] *Institut de Science des Matériaux de Mulhouse CNRS UMR 7361, Université de Haute-Alsace, Université de Strasbourg, 3b rue Alfred Werner, 68093 Mulhouse CEDEX, France; jocelyne.brendle@uha.fr
[d.] Institut Jean Lamour, UMR 7198 CNRS – Université de Lorraine, Faculté des Sciences et Technologies, B.P. 70239, 54506 Vandœuvre-lès-Nancy cedex, France.
[e.] State Key Laboratory of Chemical Resource Engineering, Beijing Engineering Center for Hierarchical Catalysts, University of Chemical Technology, No. 15 Beisanhuan East Road, Beijing, 100029 China.
[f.] Department of Materials Science and Engineering, College of Engineering, Yonsei University, Seoul 03722, Republic of Korea.
[g.] Joint Laboratory of Solid-State Chemistry, Faculty of Chemical Technology, University of Pardubice, Studentská 84, 53210 Pardubice, Czech Republic
[h.] *Department of Pharmaceutical Sciences, University of Perugia, Via del Liceo 1, 06123 Perugia, Italy; morena.nocchetti@unipg.it
[i.] Chemistry Research Laboratory, University of Oxford Department of Chemistry, 12 Mansfield Road, Oxford, OX1 3TA, United Kingdom.
[j.] Institut de Physique et Chimie des Matériaux de Strasbourg, CNRS – Université de Strasbourg, UMR7504, 23 rue du Loess, BP43, 67034 Strasbourg cedex 2, France
[k.] * Institut de Chimie de Clermont-Ferrand, Université Clermont Auvergne, UMR CNRS 6296, Clermont Auvergne INP, 24 av Blaise Pascal, BP 80026, 63171 Aubière cedex, France: fabrice.leroux@uca.fr
*Corresponding authors

contributing the most in the domain of intercalation compounds (from about 3,600 articles) are - the National Science Foundation of China (NSFC) with about 18 % of the total for all agencies, - European Commission with 5.5 %, - United States Department of Energy DOE with 5.5 % and the National Science Foundation (NSF) with 4.9 %, - the Ministry of Education Culture Sports Science and Technology Japan MEXT with 4.1% and Japan Society for the Promotion of Science with 3.1 %, - the German Research Foundation (DFG) with 2.9 % and – the Conselho Nacional de desenvolvimento Cientifico e Tecnologico (CNPQ) with 2.6 % and the Coordenacao de Aperfeicoamento de Pessoal de nivel superior CAPES with 2.2 %.

As much as possible, the aim here is to unambiguously show the advantages, limitations and the possible disadvantages of intercalation compounds in responding to scientific and technological challenges. Among intercalation layered compounds (ILCs), the family of graphene, transition-metal dichalchogenides, layered double hydroxides, layered phosphates and phosphonates, smectite clays and layered silicates, perovskite-type materials, zeolites and mesoporous materials are still scrutinised and we want to give the most useful information. To achieve this, a non-exhaustive state of the art is compiled and organised into two parts. This present part covers:

- Design and synthesis strategies (e.g. modelling and prediction by increasingly fine simulation, process design, new synthetic methods, sustainable and green synthesis, scale-up processes, hierarchical assemblies, core-shell, additive manufacturing, spray, electrospinning, nanosheets, superlattice-like heterostructures);
- Energy (e.g. new generation solar cells, Li-ion batteries, H_2 storage), supercapacitors (energy grid saving, lighting and emission/shaping in polymers);

while the second part is devoted to:

- Catalysis (e.g. photo-, bio-, electro-catalysis, water electrolysis, H_2 production, fine chemicals, separations, recycling, efficiency)
- Environment (CO_2 capture, soil remediation, plant feeding)
- Health (drug delivery/release, patch, bone regeneration, biomaterials)
- Engineering Coating/Composites as polymer fillers/Cements/textiles (anti-ox, anti-corrosion, fire retardant)

This should mirror some expectations regarding future developments as well as suitable applications of intercalation compounds.

1. Design and synthesis strategies

1.1. Where do we come from and where are we going when it comes to intercalation compounds?

1.1.a. Through intercalation

Intercalation into graphite constitutes the initial discovery of intercalation chemistry. Graphite is layered amphoteric material able to host in its Van der Waals gaps both electron donors or acceptors where redox phenomenon rules the reaction-driven intercalation process. The sorption of species in porous carbons is excluded from this prospective paper and chemical reactions on the surface of (modified/doped/substituted) graphene is only mentioned in passing, as these reactions are not strictly "true" intercalation processes. Clearly, numerous applications can be retrieved for graphene and graphene-based material which are obtained from intercalation-exfoliation reactions (Hummer's method is based on an intercalation reaction), but in most cases these applications of graphene themselves do not involve an intercalation reaction. It should be highlighted that applications involving intercalation into graphitic materials mainly concern energy storage[1]purposes and physical properties of materials. Currently, this may constitute a limited field of applications for intercalation reactions into carbons. This drawback can also be seen as advantageous as numerous perspectives could be developed by researchers in this field. In the last years, synthesis of Graphite Intercalation Compounds (GIC) remains mainly obtained by Chemical Vapor Transport of metals towards graphite, even if alternative solid-liquid reactions in molten alloys or molten salts can be developed.[2] Recently, new intercalation process using sodium as catalyst has been published, which open the road to novel materials with remarkable physical properties.[3,4]

Exchange reactions and more generally involving intercalation chemistry are very often considered as the possibility of adapting the host structure to specific properties. Two-dimensional (2-D) materials have been recently reviewed[5,6,7] including layered transition metal chalcogenides.[8, 9]

Ion-exchange materials are well described in the literature, and members belong usually to a family as exemplified by the anionic exchangers such as layered double hydroxide (LDH) or the cationic exchangers such as cationic clays, alkali transition metal (bronze) oxide or metal (IV) phosphates. In some specific cases, opposite or neutral charge ions are able to be incorporated into a host structure. For the former, cation exchange reactions are reported for hydrotalcite by revisiting sulphate and alkaline cations both interleaved as found for the Shigaite mineral.[10]

An additional step uses the spatial confinement provided by the two-dimensional network. A recent review underlines the interest of using 2-D materials as nano-reactors for confined synthesis of large variety of nanostructured materials that are found promising for electro-catalytic applications.[11]

In the case of cationic clays, ion exchange reactions lead to a wide family of modified 2D-materials. Clay-based catalysts can be prepared by ion-exchange reactions.[12] In acid-activated clays, the intercalation of protons between interlayer spaces of clay is carried out by treating the solids in acid solution. As a consequence, a slight modification of the silicate layer (often related to a partial lamellae amorphization) and textural properties is obtained.[13]

However, a proper modification with different functional groups is an interesting approach to reduce the destructive effects of acid activation and to increase interface properties for a wide range of applications. [14]

Introduction of organic species and/or polymer in the interlayer space of clays results in a modification of the hydrophilic character of clays. Alkylammonium and alkyl-phosphonium cations are the main surfactants used for intercalation process.

Anionic surfactants have been also used for clay modification.[15] Non-ionic surfactants display better properties than the other surfactants because they are thermally and chemically stable, they preserve the exchangeable inorganic cations and are normally non-toxic.[16] Gemini surfactants have been also used for clay modification.[17, 18]

1.1.b. Pillared layered structure

View Article Online
DOI: 10.1039/D4DT00755G

Pillaring is a formidable process to improve textural properties (*e.g.* porosity and specific surface area), mechanical and thermal stability of clays minerals.[19] Pillared Clays (abbreviated as PILC after) have permanent porosity that is not present in non-modified clays. To avoid the collapse of interlayer surface of different types of clays (such as smectite), stable pillars are created in the interlayer space thus preserving the porosity during the hydration or dehydration process. Exchange processes are fundamental for pillaring processes. Indeed, after a preliminary activation with Na^+ cations, the solids are exchanged with a pillaring solution containing poly-(oxy)cations and/or surfactants. Then, the calcination process is necessary for the formation of stable pillared clays (Fig. 1). A homogenous distribution of pillars results in a two-dimensional channel system with a microporous structure, high thermal stability and large specific surface area compared to zeolites.[13] The mechanism of binding of pillars into the interstitial space of clay minerals is not well known. It was proposed that the removal of protons from the OH groups of the silicate layer after calcination causes a bond between the oxygen of the pillars and the cations of the octahedral layers.[13] PILCs with pillars composed by different metal oxides (*i.e.* TiO_2, ZrO_2, Fe_2O_3, or mixed Al-Fe, Al-Zr, Al-Ti species) are largely used for catalytic and environmental applications.[20,21]

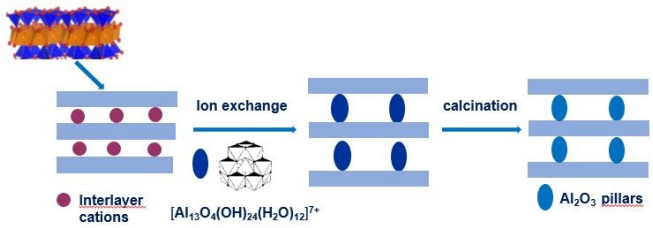

Fig. 1 Preparation of Al_2O_3 pillared clays

Porous clay heterostructures (PCHs) are a class of interesting materials that can be obtained from cationic clays and are characterised by a combination of microporous and mesoporous structure, surface acidity and cation exchange capacity.[22] The method used to prepare PCHs is the intercalation of cationic surfactant by long-chain alkylammonium into the interlayer space of smectite clay minerals, followed by the addition of neutral amine co-surfactant molecules. A silica precursor (*e.g.* tetraethyl orthosilicate (TEOS)) is then added. The 3D framework of the mesoporous silica structure between the intermediate layers of clay minerals is obtained by calcination.[22,23]

The so-called "*organoclay colloidal route*" (Fig. 2) is a novel method to prepare porous architectures from alkylammonium-exchanged smectite clays. These nanostructures can be then exploited to host metal-oxide NPs, that can be either already preformed or formed through an in-situ process.[24]

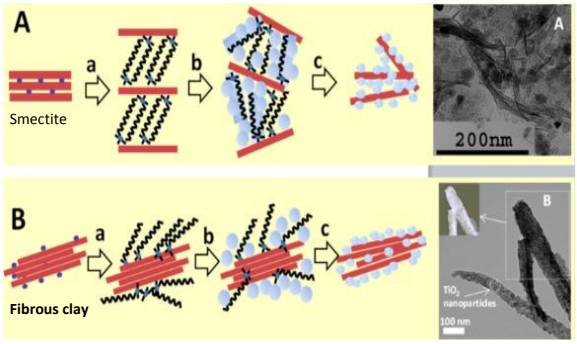

Fig. 2 Synthesis of smectites (A) of fibrous clays (B) - semiconductor nanoarchitectures by the s three step "organoclay colloidal route" : (a) formation of an organoclay thanks to the replacement of the interlayer cations by alkylammonium ions (b) treatment with metal oxide precursors and (c) calcination to obtain nanoarchitectures containing the semiconductor, reproduced with permission from Ref. 24. Copyright 2019 Beilstein-Institut.

1.1.c. Towards exfoliation

As far as bi-dimensional compounds are concerned, many efforts are attempted to exfoliate their structure and to produce single layers as reviewed for layered metal oxides and hydroxides.[25] Individual layers are suitable when there is a need to promote the surface to the bulk. With the recent emergence of graphene, efforts have been focused on its preparation by exfoliation (Fig. 3).[26a] Direct exfoliation has been reviewed to be a key solution for low-cost mass production, especially using micromechanical cleavage, sonication, ball-milling, fluid dynamics and supercritical fluid methods. However, the yield of monolayer graphene is still quite low, fragmentation effects cannot be avoided and uncontrollable defects can appear.[26b] Another possibility consists in assisted exfoliation using intercalation reaction, leading to graphene layers. The general concept is the chemical or electrochemical preparation of GIC and its consecutive exfoliation. In the latter case, depending on the nature of the guest species, a positive or negative charge transfer occurs versus graphite used as working electrode, accompanied with an oppositely charged ions intercalation. Co-intercalating molecules, especially solvated molecules, may accompany the guest species. This results in a dilation due to the increase of the interlayer spacing between graphene sheets and subsequent exfoliation depending on experimental parameters. Tunable functionalization can be operated during or after exfoliation by addition of adequate chemical agents. Anodic exfoliation involves mainly aqueous solvents with variable exfoliation yield whereas cathodic process shows higher efficiency but by damaging more the graphene sp^2 structure.[27]

GIC to form graphene can also be prepared by multi-steps process using chemical intercalation: no electrochemical cell is used, so no co-intercalated solvent molecule is involved. First, direct intercalation of potassium is realised by CVT to form the golden-brown KC_8 GIC which is then dispersed in THF. Finally, the solvent is washed/substituted with water, nevertheless the graphene material remains dispersed in the solution and a dry material is not obtained.[28] Redox intercalation into graphite can lead to graphene

oxide using the well-known Hummers methods which can be modified in order to decrease coast and free toxic gases by using other oxidative reagents and solvents.[29]

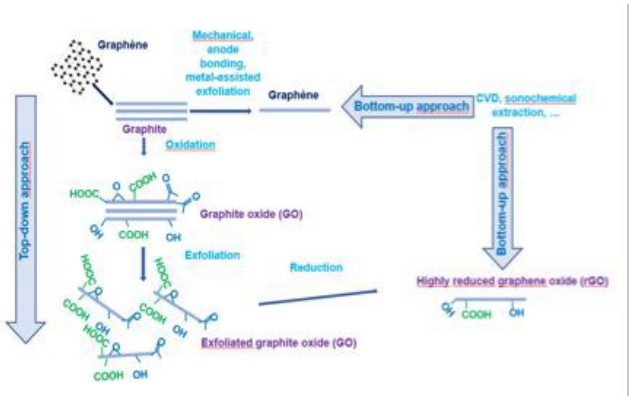

Fig. 3 Graphene derivatives, graphene oxide and reduced graphene oxide.

The combination of electrochemical intercalation and oxidation/exfoliation is also a way to produce exfoliated graphite oxide that can be subsequently treated to form Reduced Graphite Oxide (RGO) with few functional groups [30] and all processes leading to graphene materials are still reviewed[31].

Since it is not possible to intercalate graphene, because it is a monolayer, several works are attempted the intercalation under graphene, meaning between epitaxial graphene and its substrate. In most cases, the intercalation process is performed under UHV (Ultra-High Vacuum) by exposing graphene to molecular species.[32]

It should be noted a bottom-up strategy instead of the top-down approach has been developed in the last decade, especially for the preparation of N-doped graphene 2D materials, *i.e.* graphitic C_3N_4, metal-free 2D material with remarkable photocatalytic properties. The experimental procedure consists in a sequential molecule self-assembly, alcohol molecules intercalation, thermal-induced exfoliation and polycondensation process, leading to porous few-layer g-C_3N_4. Claimed as a simple bottom-up method by authors, several steps remain necessary considering the re-stacking due to reinforced π-π interactions.[33] Other ways of synthesis of such materials have also been exhaustively reviewed.[34]

Exfoliation is facilitated in the case of materials having low charge density or, in other words, when cohesive electrostatic forces that are not too strong. However, when the charge density is high, some possibilities remain as exemplified for the positively charged LDH sheets.[35] In this review, exfoliation methods and mechanisms to exfoliate are classified according to liquid exfoliation, organic molecule driven intercalation, and mechanical shearing or stirring as well as the 2D associated filler loaded to form diverse polymer nanocomposite where the interfacial interactions are the key for an efficient exfoliation. However, this usually requires a lot of solvents. The relatively small quantity of exfoliated materials per unit volume strongly limits their application and thus often remains a laboratory feat with no real technology transfer possible. Another point of attention is that the exfoliation leading to the total exposure of the inter-lamellar species is not desired in many cases. The de-cohesion of the structural stack leads to the possible migration of guest species.

Exfoliation of cationic smectites (*e.g.* montmorillonite) can be achieved in both polar and non-polar solvents.[36]

In aqueous environment, the interlayer exchangeable cations are surrounded by water molecules, thus increasing the interlayer distance. In diluted suspension clays can naturally dissociate into particles that can be then partly or completely exfoliated. These processes strongly depend on the concentration of clays suspension, and on the type of cations present in the interlayer space. An organic modification is needed for the exfoliation in nonpolar media, leading to transform the hydrophilic surface into a hydrophobic one and to increase the interlayer space of clays. The exfoliation degree is influenced by several factors such as the nature of the organic species and the degree of organic modification, the polarity and the chemical nature of the solvent.[36]

1.2. For a better particle size control

Alongside exfoliation, the controlled synthesis of small particles is also strongly desired. To do so, the bottom-up preparation of ultrathin LDHs assisted by a reactor is a promising strategy. Previously, Duan and co-workers developed the separate nucleation and aging steps (SNAS) method using a commercial colloidal mill reactor to facilitate the scale-up preparation of nanostructured LDHs.[37] This method utilises forced micro-mixing technology to rapidly blend the metal salt solution with the alkali solution in the gap between the rotors. Nucleation of the particles occurs within a matter of seconds, resulting in LDH nanosheets that possess a small and uniform particle size ranging from 60 to 80 nm.[38] Therefore, attempting to add a laminar inhibitor in the reactor-assisted synthesis process of LDHs may potentially inhibit the growth of LDH in the Z-axis direction, resulting in the formation of ultra-thin LDH. Formamide, a stable lamellar inhibitor, can be adsorbed on the LDH layer and suppress the growth of LDH in the Z-axis direction. The monolayer LDHs with a thickness of ~1 nm was obtained by modifying the industry colloid mill reactor through the addition of a small amount of layer growth inhibitor formamide using SNAS method.[39]

Another way that is also complicated to implement consists in using so-called topochemical reactions. It is nicely illustrated by recent hetero-structures obtained from the ingress of Cu(I) into vacancies of the layered crystalline structure of Fe_7S_8 hexagonal nanoplate.[40] The topochemical reaction is also reported for anions. Known since decades for mobile oxygen anions, the topochemical reaction is reported for chalcogen anions and proceeds through de-intercalation reaction from stable pristine materials as exemplified by layered cobalt chalcogenides leading to new metastable compounds[41] or oxy-chalcogenide where the insertion of copper is

DOI: 10.1039/D4DT00755G

acting with chalcogen dimers redox reaction.[42] In the latter it is illustrated with the de-intercalation/re-intercalation of sulphur in the layered oxy-chalcogenide $La_2O_2S_2$ for which structure prediction and electron microscopy help to understand its topochemical soft chemistry reaction.[43]

More applicative, topochemical insertion and desorption reactions are applied to mobile ions in the prospect of next-generation energy storage mechanism. Fluoride anions (de)intercalation is reported in a Ruddlesden-Popper type perovskite $LaSrMnO_4$ by substituting of oxygen atom in the apical sites with fluorine yielding to oxyfluorides of interest as cathode.[44] Similar de-fluorination is reported for $Sr_2TiO_3F_2$ as anode in fluoride-ion battery.[45]

In other cases, the topochemical reaction proceeds by dissolution of a pristine host structure followed by nucleation and growth rather than by transient solid-state intercalation. Thus, the filling of sites that are nevertheless vacant and therefore available does not take place by migration into the structure but through a dissolution-reprecipitation front as elucidated with the transformation of gibbsite into LiAl-LDH by multinuclear NMR [46] or the transformation from layered single hydroxide (LSH) in layered double hydroxide (LDH) by using solid state kinetics formalism.[47]

1.3. Let's exemplify zirconium phosphate (ZrP)

Zirconium phosphate (ZrP) is an interesting cationic exchanger of which several chemical method, such as refluxing, hydrothermal, sol-gel, microemulsion and microwave method, can be used to synthesise amorphous or crystalline phases of ZrP.[48] All these mentioned synthetic strategies involve the addition of phosphate to a solution of zirconium (IV) salt, often in the presence of complexing agents such are HF[49] oxalic acid[50] and formamide[51] resulting in precipitation of amorphous or crystalline ZrP. The choice of preparation method and reaction conditions strongly influences not only the degree of crystallinity, but also the shape and size of the particles. Now chemists are trying to develop more environmentally friendly methods, which avoid the use of excess acids and complexing agents. Several solid-state methods using various alkali metal phosphates were developed. Flower like α-ZrP was obtained by grinding $ZrOCl_2{\cdot}8H_2O$ together with Na_3PO_4 followed by hydrothermal treatment.[52] Bevara *et al*. synthesised highly crystalline $K_2Zr(PO_4)_2$ by heating of pressed pellets containing ZrO_2 and KPO_3 at 750°C.[53] Minimal liquid approach, in which reagents are mixed in their as-obtained state and concentration, was used for synthesis α-ZrP.[54] $ZrOCl_2{\cdot}8H_2O$ was mixed with concentrated orthophosphoric acid (P/Zr = 2 or 3) and heated at 25 - 120°C for 24 h. Larger crystals were obtained at higher P/Zr ratio and the crystallinity of the sample increases with increasing reaction temperature. If a small amount of fluoride ions was added into the reaction mixture, the highly crystalline product was obtained and the its morphology changed from platelets to rod-shape particles with increasing F/Zr ratio. A highly crystalline γ-ZrP can be obtained using NaH_2PO_4 instead of orthophosphoric acid.[55] Similarly, α-$Zr(NH_4PO_4)_2{\cdot}2H_2O$ can be prepared using $ZrOCl_2{\cdot}8H_2O$, $(NH_4)_2HPO_4$ and a small amount of Na.[56]

Another direction in the development of methods for ZrP synthesis is the preparation of material with properties tailored to the specific application, especially ZrP with high specific surface and suitable porosity for ion-exchange and catalytic application. So called template method using surfactant that can be cationic (e.g. cetyltrimethylammonium[57] or tetradecyltrimethylammonium[58]bromide) anionic (sodium dodecylsulfate [59]) or neutral (e.g. Brij56 [60] pluronic P123[61], triton-X[62]) to precipitate ZrP followed by a calcination seems to be very useful. Tian and coworkers synthesised mesoporous ZrP using yeast cells as a template.[63]Another way to synthesise mesoporous ZrP is from the calcination of zirconium phosphonates.[64] An interesting paper, describing preparation of ZrP with different morphologies, rod-like (minimalistic method), spherical (surfactant templating) and cube-like (sol-gel), was published in 2020.[65] Highly porous monolithic zirconium phosphate was prepared by sol-gel synthesis in the presence of poly(ethylene oxide) and poly(acrylamide) followed by supercritical drying.[66a,b] In this case, the presence of both polymers is necessary to form a macroscopic structure with the macropore size controlled by changing the ratio between polymers and orthophosphoric acid.

The growing interest in nanotechnologies is leading to the development of new methods for the synthesis of nanoparticles with a controlled shape and size. Hajipour and coworkers prepared hexagonal α-ZrP nanoparticles using poly(vinyl alcohol) or polyvinylpyrrolidone in water solution.[67] Hexagonal nanocrystalline ZrP particles were formed by addition of H_3PO_4 to the alcoholic solution of zirconium propionate.[68] Dried samples have α-ZrP structure with intercalated alcohol. By heating of this sample to 120 °C, a new phase with 3D structure consisting of cube-like nanoparticles was obtained.[69] This phase was called τ´-$Zr(HPO_4)_2$ due to its structural similarity with already known τ-ZrP. Recently a microwave assisted hydrothermal method was used for synthesis of hexagonal ZrP nanodiscs.[70]

Single-layer α-ZrP nanosheets can be also obtained so called "top-down" method i.e., by exfoliation of already synthesised ZrP using various chemicals and solvents. The ways of ZrP exfoliation have been reviewed recently.[71] A widely used amine for α-ZrP exfoliation is propylamine or methylamine.[72] Recently, exfoliation of α-ZrP using allylamine was described.[73] Alkanolamines can also serve as exfoliating agent, the minimum amount necessary for exfoliation is less than that of monoamine. [74]Other agents widely used for α-ZrP exfoliation are tetraalkylammonium hydroxides.[75] The aqueous exfoliation is most common, but the dispersion of nanosheets in an organic solvent is desired for many applications. Replacement of water for desired organic solvent can be realised after exfoliation through multiple cycles of centrifuge-rinse or by heating for high-boiling point organic solvents. Exfoliation can be also achieved by intercalation of excessively large amine[76] such as poly(ether)amines with molecular weight of about thousand g/mol, or intercalation of

large amines followed by the intercalation of polymers.[77] Main drawback of using poly(ether)amine is the difficulty to be removed from the medium, but an exfoliation state can be reached in organic solvents. For instance, nanosised α-ZrP prepared in methanol[78]can be directly exfoliated in methanol.[79]

1.4. Welcome to a new family: the MXenes

While intercalation compounds have been known for decades or centuries, some of them are revisited and others are synthesised more recently as Carbon nanotubes 1D-compounds and Metal Oxides Frameworks (MOF) 3D-compounds, in the early and late 1990's, respectively, MXenes 2D-compounds in the 2010's.

A little more than a decade ago, the latter family of intercalation compounds MXenes emerges with the synthesis of Ti_3C_2 from the leaching of Al from Ti_3AlC_2 in an aqueous HF solution. Since then, these materials are always studied for their fabulous properties related to their 2D structure, their adjustable bandgap and the richness of their surface chemistry among others as underlined in the highly cited review.[78]

Such 2D intercalation compounds composed of transition metal carbides, carbo-nitrides and nitrides are of interest for interlayer engineering and the associated host-guest intercalation chemistry[79]and in particular for electrochemical energy storage applications mostly as electrode materials in supercapacitors and rechargeable batteries due to their high electrical conductivity allowing higher power density.[80]

Unit blocks obtained from topochemical reactions or from MXenes may form heterostructures such as $Ti_3C_2T_x$/C/MoO_2 microspheres, 2D/2D/0D heterojunctions to fine tune the electric/dielectric properties for wave absorption and shielding.[81]

Despite the very high potential of MXenes, the use of HF in the etching process poses a serious problem for large-scale manufacturing as well as to produce high quality crystals. Therefore, synthesis pathways are explored as deposition by chemical vapour or by plasma enhanced pulsed laser.[82] MXene-based core-shell nanocomposites have also been investigated using core-shell MXene functionalised with carboxylate groups interacting with PEI/PAA in contact with gold nanoparticles for application in catalysis.[83]

2. Energy

2.1. The interest of ILCs seen by machine learning methods

Since their layered structure may be propped apart either van der Waals or not interlayer space can accommodate more or less cumbersome guest species. In the literature it is well demonstrated in organic-inorganic hybrid materials where the host layered structure is used as a cargo to protect, deliver or rather prevent from migration its moieties as shown in the companion article (part 2). As far as energy domain is concerned, such tunability in the interlayer domain size is of interest for new technology beyond LiB adopting bigger size cation or anion, since the diffusion in and out of the guest is not limited by the size of the vacancies such as in tunnel or canal voids-based open structures. A recent article reviews the reason why some 2D-materials including transition metal oxides, chalcogenides, carbides and nitrides to perform efficiently as positive electrode materials in a large range of batteries (AIB, dual batteries).[84] Another review points out the importance to select guest species from an interlayer engineering point of view to improve selective ion separation membrane and ion storage performance in battery.[85]

Indeed, intercalation layered materials inherent of their versatile open structure are considered as challenging solution for the design of new energy concept. Performing computational science by using first-principles calculations on more than 9 000 compounds as well as machine learning, a recent study helps to better understand the reason of layered compounds stability or instability upon intercalation and de-intercalation process.[86] Other machine learning methods provide insights for 2D-material developing a binding energy and structural accommodation-based classification model to screen anode materials for next-generation batteries,[87] when confronting the 2D topology and their inherent heterostructure with the grain boundaries that facilitate surface adsorption site of Na^+ cations for the same application in NIBs [88] or to find «universal design strategy» for cathode materials that should be air stable such as O3 layered oxides.[89] Such predictive understanding the stability toward host-guest possibilities using first-principles calculations are often applied to energy storage application to better understand the mechanisms as well as predicting virtual structures to synthesize or to modulate the host-guest interaction by changing the nature of its ligands for a specific demand regarding the reversibility of the electrochemical intercalation process.[90]

Among intercalation compounds, 2D materials present open structure for fast ion diffusion and charge transport suitable for electrochemical energy storage and electro-catalysis as recently reviewed[91]and their role as filler in polymer composite electrolytes (PCE), as either active ion conductive or passive no ion conductive. Such inorganic platelets may be graphene oxide, boron nitride, transition metal chalcogenides, phosphorene, MXenes and 2D layered clay minerals, such as layered double hydroxides and silicates (vide infra).[92] This review emphasises the benefit of using 2D materials for PCE in lithium as well as in post-lithium batteries. Another review reports on GO/LDH and GO/Mxenes for the different types of energy storage as LiS, NIB, KIB and supercapacitor underlining the importance to combine materials in order to have interconnected network of 2D/2D materials thus preventing layers agglomeration and thus promoting the ion mass transport.[93]

2.2. Li ion batteries: LiB

For the former, although the field of lithium-ion batteries is now very mature in terms of electrode materials and this technology has been transferred and commercialised[94], significant advances are still being made in intercalation chemistry to identify possible « beyond Li battery» technologies since its limits can now be exceeded by other, less affected by the rarefaction of its elements.

At the anode, due to its superior performance including high practical specific capacity provided (360 mA.h.g^{-1} *vs.* theoretical 372 mA.h.g^{-1}), low operation potential (0.1 V *vs.* Li$^+$/Li), reversible capacity, graphite remains among the best anode material in the Li-ion battery technology (LIB). Lithium intercalation into graphite is maybe the most famous example of intercalation reaction involved for energy purpose and has been (once again) recently reviewed. Considering graphite as anode in LIB, ambient temperature, particle size and morphology as well as the electrode engineering are impact parameters still challenging [95, 96]

The advantages and drawbacks to use synthetic versus natural graphite are also under debate, as well as lithium diffusion coefficient in the carbon matrix depending on the stage GIC for high-rate applications. In LIB, lithium intercalation into graphite occurs together with Solid Electrolyte Interphase (SEI) formation whose stability is a key point for aging and safety issues. As perspective, recycling processes constitute a part of the future of graphite intercalated by lithium as its recovery is a promising route in order to circumvent mining of natural graphite that is becoming a critical resource.[97] Staging intercalation of lithium into graphite accompanied with the Daumas-Hérold picture is well known (Figure 4), but some planar structural mechanism remains controversary in the recent literature.[98]

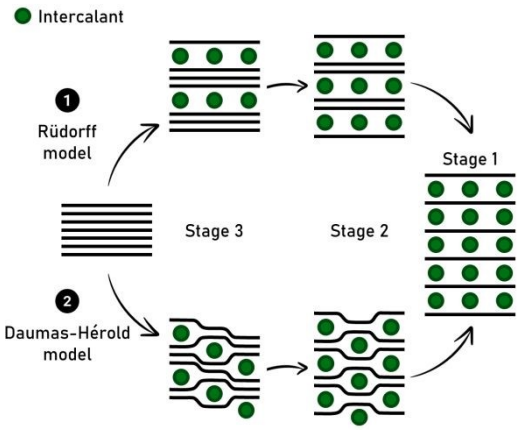

Fig. 4 Schematic representation of Rüdorff model versus Daumas-Hérold model, taking into account the flexible feature of graphene sheets. Such a model allows to describe the continuous transformation from third to second stage GIC.

So, staging phenomenon remains to be fully elucidated and appears more complex than expected and complementary *operando* techniques and *ex-situ* analyses should be explored as pointed out in a recent study of Komaba and co-workers concerning K-ion batteries.[99] In this technology, graphite remains a promising material and intercalation reactions need to be investigated further (see after).

At the nanoscale, outstanding properties have been expected for graphene as a promising material for electrochemical energy storage applications. But graphene single layer cannot be intercalated, and considering LIB, the most promising result could be obtained by Li$^+$ adsorption on both surface of the layer to form Li_2C_6 with theoretical capacity of 744 mAh.g^{-1}. However, defects formed during graphene synthesis and very high surface area blemish this ideal picture and make graphene-based cells unfeasible for alkali-ion technology.[100]Chemical doping of graphite, graphene or few-layers graphene is also an envisaged strategy in order to improve the affinity between alkali ions and the carbon matrix in corresponding batteries.[101]

The interest of ILCs is observed in the case of fast-charging as reported for Li-based anode materials using vanadium-based oxide.[102] The conductive open network is based on an inherent heterostructure formed by the stacking of two vacancy-ordered types of sheets interleaved by either Na$^+$ or Mg^{2+} cations leading to large spacing that helps the diffusion process while enhancing the electronic conductivity in the vicinity of the vanadium redox sites through a rapid multi-electron reaction behaving as a pseudocapacitive redox surface in the inner open structure.

Clays are also used to prepare electrode materials for rechargeable metal-ion batteries. One reported strategy is to use them to prepare high-capacity Si anodes as, in view of an up-scaling of the production, it is more convenient to extract silicon from earth-abundant or marine abundant (pelogic clays) eco-friendly and low-cost sources rather than from synthetic silica. Starting from natural halloysite, Zhou et al. (2016)[103] prepared interconnected Si nanoparticules through selective acid etching of halloysite enabling then removal of alumina sheets followed by magnesiothermic reduction at 700°C with the assistance of NaCl processes. Thanks to the small particle sizes (in the range 20–50 nm) and the porous structure this new Si anode exhibit satisfactory performance as an anode for LiB with a specific capacity of 800 mAh g^{-1} at a current density of 1C after 1000. Magnesiothermic reduction was also applied starting from montmorillonite[104], talc [105,106], Laponite®[107], vermiculite[108], attapulgite[109] as well as pelagic clays.[110] In the case of talc, by fine tuning the preparative methods, a mixture of Si and SiO_2 particles having sizes going from tens to hundreds nanometres were formed.[105]The addition of a carbon layer on these particles imparts electronic conductivity as well as improved durability towards stresses associated with the volume change of Si/ SiO*x* during cycling. In the same way, pelogic clays and sucrose were used as source of silicon and carbon to form a carbon-coated porous silicon anode

demonstrating performance with a specific capacities of 540 mA/g under the current density of 0.5 A.g^{-1} after 120 cycles.[110]

Si nanosheets possessing hierarchical porous structures were also obtained from vermiculite through a mild (300°C) and low-cost strategy involving a chemical delamination, acidification and low-temperature aluminothermic reduction in a eutectic molten system.[111] The formation of Si nanosheets was explained by the self-templating role of the vermiculite assisted with subsequent mild reduction reaction. High lithium-storage properties were obtained with a reversible capacity as high as 1269 mAh.g^{-1} at 1.0 A.g^{-1} after 300 cycles and excellent rate capability with desirable capacities of 1314 mAh.g^{-1} at 4.0 A.g^{-1}. Porous silicon/carbon composite nanosheets were also fabricated by reducing the carbon-coated expanded vermiculite with metallic Al in the molten salts.[112] Under these conditions, the layered structure of vermiculite was retained with a thickness of less than 50 nm and the formed carbon nanolayer serves as the diffusion barrier and mechanical support for the growth of mesoporous silicon nanosheets. Remarkable electrochemical performances are displayed by this anode, as a reversible capacity of 1837 mAh.g^{-1} at 4 A.g^{-1} and retaining 71.5% of the initial capacity after 500 cycles are observed.

Attapulgite and polyacrylonitrile (PAN) were also used to form nano-sized attapulgite-based aerogels. It was demonstrated that the carbonised AT-based aerogels used as active anode materials of LIBs, exhibited average discharge capacity of 534.6 mAh g^{-1} at 100 mA g^{-1} after 50 cycles.[113]

A relationship between the type of clay and the morphology of the resulting Si has been established by Chen et al.[104] Attapulgite leads to the formation of 0D nanoparticles, whereas Si derived from showed a 3D interconnected framework and 2D nano Si stemmed from montmorillonite, vermiculite, indicating that in this case, the original morphology is maintained.

Beside using clay-derived silicon and silica anodes, iron oxide-carbon-clay nanocomposites are also good candidates for LIBs as demonstrated by Alonso-Domínguez et al.[114] Using an environmentally friendly process involving sepiolite bentonite, oxyhydroxide-type phase, FeOOH, sodium alginate and glucose composites having high-capacity values of ~2500 mAh.g^{-1} after 30 cycles at 1 A.g^{-1} and retentions close to 92% are obtained. Sepiolite based composites display an outstanding cycling stability interpreted in terms of an optimal interaction between iron oxide nanoparticles and sepiolite surface through hydrogen bonds, related to the particular structural and compositional features sepiolite.

At the cathode, from common alkali-rich layered cathode materials $Na_z[Li_xMn_y]O_2$, close comparisons between similar compositions have identified the cause of the first charge hysteresis with O^{2-} oxidised and then cleaved in discharge.[115] The authors scrutinise the honeycomb superstructure arising from the local ordering of lithium and transition metal ions during first cycle and note that the presence of such superstructure prevents the migration of manganese ions and therefore the loss of energy density.

Even if original approaches are still developed such as misfit layer heterostructure SnS/TiS_2 studied as superior anode material for LIB and based on a conversion-alloy mechanism upon lithiation/delithiation.[116]

However, on the whole, the current LiBs technology is stalling today because the capacities at the cathode but also at the anode are limited.

2.3. Li-S batteries

Compared to traditional carbon cathode, Li-S batteries have gained growing number of attention and are considered as one of the most promising next-generation energy storage systems owing to their remarkably high energy density (2600 Wh.kg^{-1}), earth abundance of sulfur and large theoretical specific capacity (1675 mAh.g^{-1}). Clays are excellent candidates to circumvent the drawbacks of sulfur cathodes.[117,118] Indeed, their interlayer space can accommodate the volume of expansion of sulfur cathodes, the dissolution and shuttle effect of polysulfide can be suppressed by the confinement of the sulfur cathode in different clays (montmorillonite, halloysite) and clays-sulfur cathodes permit free transportation of lithium, resulting in efficient and straightforward ion diffusion.[119] As an example, a Li-montmorillonite-sulfur cathode prepared by a simple process including the incorporation of 80 wt% of sulfur powder demonstrated high capacity and nearly sulfur loading-independent cell performance.[118] Sulphur infiltrated in vermiculite leads to cathodes demonstrating outstanding rate capacity and cycling stability.[120] In this case, it was concluded that thanks to the cations present at the surface of vermiculite, polysulfides anions (S_n^{2-}) can be adsorbed, thus preventing them from dissolution, moreover, it was assumed that the excess surface charge is most probably compensated by excess Li^+ in the space charge zones which is beneficial for charge transfer and local conductivity. A comparison between the performance of this cathode and regular carbon-sulfur based cathodes revealed that promising rate capability as well as much better cycling stability are obtained with vermiculite-sulfur cathodes, showing all the potential of clays as host for sulfur and formation of high-performance cathode for lithium-chalcogen batteries. Conductive polymer coated onto LDH provides a suitable volume to reserve the lithium polysulfides (LiPSs) thus increasing the kinetics of sulfur-based redox reaction.[121] Polypyrrole associated with LDH platelets improves the electrode performance by preventing the shuttling of LiPSs. In the same vein, it is found that LDH cations act as sulphur host and in particular NiFe by interacting with LiPSs, resulting in better performance of the LiS battery.[122]
Beyond intercalation, conversion is also possible for a large number of electrode materials that can have very large theoretical capacities. Conversion-type materials in particular transition metal fluorides and sulphides are reported as high-energy density anodes and cathodes.[123]

2.4. Beyond LiBs technology using ILCs

New trends are also emerging to find breakthrough solutions with expanded concepts of intercalation chemistry pushing materials to their limits to have sufficiently open structures. In addition, the following inventory which is intended to be non-exhaustive, thus includes solutions to compensate for the scarcity of the elements that make up lithium batteries (LIBs) such as cobalt, nickel, copper (as current collector) and lithium. Even graphite is becoming a critical material. These are Na- (NIBs), K- (KIBs), aqueous Zn- (ZIBs) ion batteries.

2.4.a. NIBs and KIBs

NIBs and KIBs appears more and more as promising alternatives to secondary LIBs. Inspired by the knowledge on graphite as anode and layered oxides as cathode in LIB, breakthroughs have been demonstrated in Na-ion and K-ion batteries based on experimental and theoretical calculations. It is worth noting that differences exist in interfaces and host-guest interactions depending on the electrolyte (*i.e.* alkali ion and solvent molecules), so that a direct transfer of LIB technology to NIBs and KIBs is simplified but remains complex. At the anode (disordered carbon which are not layered materials are excluded from this perspective paper), the stability of the pseudo fully intercalated alkali-based GIC with lithium, sodium, or potassium has been determined by thermodynamic approach considering numerous interactions in pristine and intercalated materials. This stability explains why sodium is not easily intercalated into graphite. However, the nature of chemical bonds in these GIC remains controversy. Moreover, it appears clearly that the nature of the electrolyte is a fundamental parameter for regulating the aforementioned interactions. With some systems, a binary alkali-GIC can be obtained; considering particular electrolytes (with diglyme-based or ether-based) co-intercalation of solvent and solvated ions occurs simultaneously and stabilises Graphite Co-intercalation Compounds.[124] For instance, it makes possible the intercalation of sodium into natural graphite.[125] In the future, strategies for achieving favourable intercalation of alkali metal ions into graphite could be based on the introduction of heterogenous species (covalent or non-covalent functionalization of graphite, carbon atoms substitution, use of GIC as starting point), the modification of the morphology or the elaboration of novel solvents for co-intercalation phenomena.[126] Thanks to a multi-tools approach, it was proposed that the use of well-selected solvents such as ethers allows the co-intercalation of Na ions and ether molecules, the latter screening the repulsions among charge-carriers ions.[127] However, co-intercalation of solvents causes a high level of volume change, inherently limiting its practical application and a survey on recent developments of carbon-based and alloy-based anodes for NIBs is a way to solve this issue.[128] The use of graphene heterostructure is also investigated as alternative electroactive materials in batteries. Sun *et al.* showed that a hybrid material made of alternate graphene and phosphorene layers can drastically increase the specific capacity of the anode thanks to an intercalation-alloying mechanism together with mechanical-electrical synergic effects.[129] Such heterostructure can constitute a suitable anode for NIB technology.

Graphite can also be involved as anode in K-ion battery rising technology using liquid organic electrolyte at room temperature but it shows moderate rate capability and relatively fast capacity fading related to the dramatic volume expansion after intercalation into van der Waals galleries (interplanar distance increases from 335 pm for pristine graphite to 535 pm for KC_8 1st stage GIC). It is necessary to transpose knowledge about LIB and NIB technologies to KIB technologies, but developments are mandatory concerning the nature and structure of the anodic carbon material, the involved intercalation mechanisms, the composition of the electrolyte.[130]

It is our belief that new emerging materials or revisited well-known composition should reach some of the requirements to go beyond LIBs technology. For instance, building blocks approach is a fascinating synthesis to vary the stoichiometric combination of redox metal, as recently illustrated by the 2D non-van der Waals layered materials $Li_2MP_2S_6$.[131]

In order to improve the low-rate capacity and poor cycling stability inherent to 2D ternary metal phosphorus, defects are introduced into $MnPS_3$ layers as well as the presence of interleaved species such as cations methylammonium Me_4N^+, tetraethylammonium Et_4N^+ or pyridine PyH^+ yields the hybrid layered compound: $Mn_{1-x}PS_3y_{2x}$ (y = Et_4N^+, Me_4N^+, pyH^+).[132]

The Na^+ energy storage mechanism of $MnPS_3$ follows (according to the XRD phase identification in Figure 5):

$MnPS_3 + 9Na^+ + 9e^- \rightarrow 3Na_2S + Na_3P + Mn$ (in discharge)

$Mn + Na_2S + Na_3P - 5e^- \rightarrow MnS + P + 5Na^+$ (in charge)

$MnS + P + 5Na^+ + 5e^- \leftrightarrow Mn + Na_2S + Na_3P$ (upon cycling)

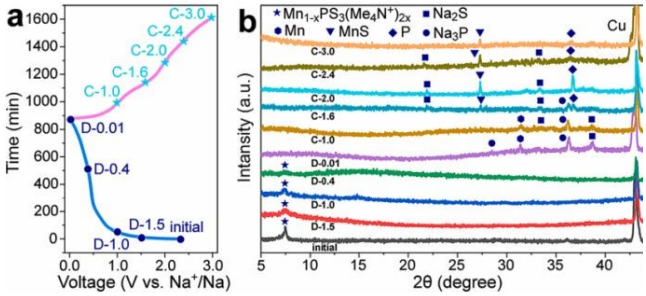

Fig. 5 (a) The initial charge–discharge curve of the $Mn_{1-x}PS_3(Me_4N^+)_{2x}$ electrode at 0.05 A/g, and (b) the corresponding ex-situ XRD patterns at various voltage stages. Reproduced with permission from ref. 132. Copyright (2024) Elsevier.

Intralayer defect vacancies engineering by CVD are found to create electronic conductivity, and the expandable spacing suitable for the rapid diffusion of the Na^+ cations as well as to mitigate the material volume expansion upon intercalation and deintercalation when used as electrode materials in NIBs: $Mn_{1-x}PS_3y_{2x}$ hybrid composite electrodes exhibit higher specific capacity and rate performance than $MnPS_3$ electrode (Table 1) and interestingly $Mn_{1-x}PS_3(Me_4N^+)_{2x}$ with

View Article Online
DOI: 10.1039/D4DT00755G

a larger interlayer distance in the series exhibits the higher specific capacity due to a better access of the electrolyte as reported by the authors.

Due to the high redox potential of $V^{4+}/^{5+}$, vanadium-based materials are considered as electrode materials in NIBs. Interestingly the authors focus on vanadium-based phosphate $AVOPO_4$ and use $KVOPO_4$ commonly employed in KIBs but in NIBs.[133]The small part of K^+ remaining after the exchange K^+ for Na^+ for the first cycles is found to have a «pillar» effect thus facilitating the diffusion kinetics and reversible storage of Na^+ cations, and finally completely outperforming $NaVOPO_4$ (Table 1).

In the strategy that interleaved species may act actively to perform better than the pristine compounds, some studies report the intercalation of ethylene glycol in 1T/2H-$MoSe_2$ leading to a 1T phase percentage as high as 80 %.[134] Ethylene glycol is used as sacrificial guest to produce an interstratified conductive layer, thus helping in connecting electronically the entire materials as well as preventing the restacking of $MoSe_2$ upon intercalation/deintercalation cycle. Used as anode in NIBs, the performance of the composite hybrid layered material 1T/2H-$MoSe_2$@C is appealing in terms of energy and capacity retention (Table 1).

Two subsequent intercalations between $TiSe_2$ induce the delamination of the platelets in well exposed nano-sheets that exhibit low diffusion barrier towards Na^+ cation diffusion.[135] Propylamine then followed by hexamine insertion leads to a spontaneous exfoliation of the layered structure. A rapid electrochemical reaction in NIB is observed due to the fact that the redox active sites are well exposed, combining an efficient inner-wettability of the electrolyte, a stability of the structure. All these result in a high specific capacity associated to the low polarization (Table 1). From TEM, ex situ XPS and CV, the mechanism of both sodiation and desodiation processes is found to proceed in two-step, intercalation and conversion as follows (V *vs*. Na^+/Na):

$$TiSe_2 + xe^- + xNa^+ \rightarrow Na_xTiSe_2 \quad (1.62)$$
$$Na_xTiSe_2 + (4-x)e^- + (4-x)\,Na^+ \rightarrow Ti + 2\,Na_2Se \quad (1.0\text{ V}) \,\&\, (0.6\text{ V})$$

$$Ti + 2\,Na_2Se \rightarrow Na_xTiSe_2 + (4-x)e^- + (4-x)\,Na^+ \quad (1.5\text{ V})$$
$$Na_xTiSe_2 \rightarrow TiSe_2 + xe^- + xNa^+ \quad (1.9\text{ V})$$

It was possible to index by HRTEM the lattice fringes (400) of Na_2Se, which is lamellar.

Topochemical reaction may affect the insertion of big-size mobile ions such as in KIBs. Indeed, in addition to the interlayer space, the intralayer domain is rich in terms of substitution for many families of layered structure, thus leading to almost infinite possible combination. Such versatility is largely reported in the literature for $LiNi_xCo_yMn_zO_2$ known as NMC layered structure using some Al^{3+} cations substitution to stabilize structurally the structure. A recent example reports the use of $K_xCr_{0.75}Ti_{0.25}O_2$ instead of K_xCrO_2 as cathodes for KIBs.[136] Such topochemical exchange reaction stabilizes usually the pristine layered structure upon charge/discharge cycles and this example shows that layered structure can be diversely modified to new technology.

Another approach is to interstratify sheets of layered structure. It is recently reported by using a unique intergrowth of the same composition but presenting different stacking sequence, resulting in a biphasic P2/P3 of $K_{0.7}Mn_{0.67}Ni_{0.33}O_2$ composite.[137] This composite shows a high energy density and capacity retention when used as cathode in KIBs.

Clay-based silicon and silica anodes have also attracted attention in the recent years for applications in NIBs and KIBs but it was shown that their there are not suitable candidates for these applications.[138] More interesting are composites prepared by wrapping of halloysite with a conductive a layer of polypyrrole (PPy) via in situ polymerization. Indeed, in this way, a cathode material able to maintain a capacity of 126 mAh g^{-1} after 280 cycles at current density of 200 mA.g^{-1} is obtained.[139] Sodium-montmorillonite was also use as sodium–ion–conductor interface in a sodium-based composites anode prepared by a mechanical mixing of sodium and sodium montmorillonite. The use of sodium montmorillonite enables in particular, providing sodium diffusion channels, the reduction of the nucleation potential of sodium and reduce the generation of sodium dendrites during repeated plating and stripping process of Na. Excellent cycling performance and favourable rate capability in both carbonate and ether electrolytes were obtained.[140]

In NIBs new intercalation compounds are also considered such as MXene $Ti_3C_2T_x$ exhibiting reversible Na^+ intercalation/deintercalation in a nonaqueous electrolyte and a good capacity retention upon cycling.[141]

Grafting azobenzene sulfonic acid (ASA) onto V_2C MXene induce an expansion of the interlayer space which is a benefit for the specific capacity as well as for the rate capability in KIB.[142]

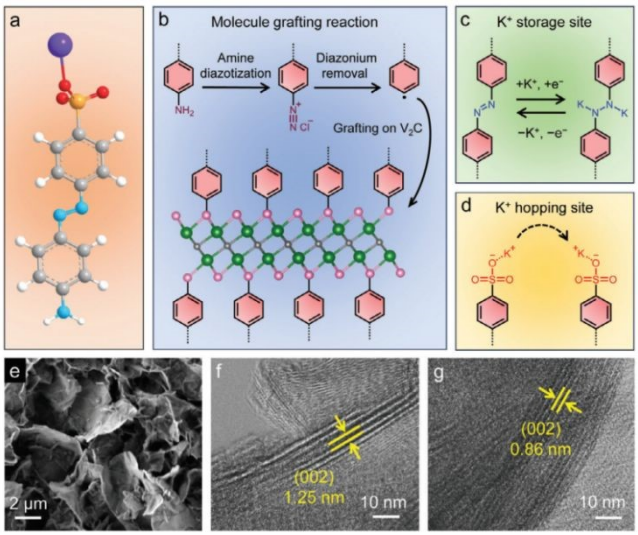

Fig. 6 Schematic illustration showing a) 4-aminoazobenzene-4'-sulfonic acid sodium salt (white sphere: H; grey sphere: C; blue sphere: N; orange sphere: S; red sphere: O; purple sphere: Na), b) molecule grafting reaction (black sphere: C; green sphere: V; pink sphere: the terminals of V_2C MXene), c) the azobenzene unit as the extra K^+-storage site, and d) the sulfonate anion as the K^+-hopping site. e) Scanning electron microscopy image of ASA-V_2C nanoflakes. HR-TEM images of f) the ASA-V_2C film and g) the pristine V_2C film. Reproduced with permission from Fig. 142. Copyright (2024) Wiley-VCH GmbH.

The better performance of ASA V_2C compared to V_2C is explained on the basis of hopping site for K^+ cations at the sulfonate anion and an extra storage site at the azobenzene unit in addition to the V_2C layers response (Figure 6).
It is also demonstrated by synchrotron operando XRD that the organic moieties alleviate the structural distortion upon K^+ intercalation and de-intercalation that is strongly visible for V_2C and not ASA V_2C.

2.4.b. ZIBs and MIBs

Electrode and electrolyte materials for KIBs have been recently reviewed.[143]as well as for ZIBs.[144,145] An expandable interlayer space as well as the possibility to be delaminated make them of interest to be revisited as electrode materials adopting a technology with big-size mobile ions. This is nicely exemplified by the recent advances concerning δ-MnO_2, layered manganese dioxide that permit to investigate them as cathode in AZIBs on the contrary to all the other MnO_2 (α-, β-forms and hollandite that are based on rigid canal open-structure.[146] Layered δ-MnO_2 materials are pre-intercalated with bulky organic species (benzene-based functionalized cation) leading to a large expansion of the spacing. Guest molecules are considered as «supportive pillars» supplying stability as well as to increase the diffusion process of Zn^{2+} cations intercalation and reverse desertion, altogether showing much better electrochemical performances compared to the pristine δ-MnO_2.

In the same vein using δ-MnO_2 as cathode in AZIBs, birnessite manganese oxide is co-intercalated by sodium and copper.[147] The co-intercalation is found to boost the electrochemical performances due to an activation effect of Cu^{2+} on the Mn^{2+}/Mn^{4+} redox pair on the surface, and Na^+ cations stabilize the host structure during the two-electron transfer reaction occurring in AZIBs.

Intercalation of inorganic redox centres is reported for vanadium oxide and their potential use in aqueous zinc-ion batteries AZIBs.[148] In this study, $Mo_3V_{15}O_{35}{\cdot}nH_2O$ nanosheets are obtained using a one-step hydrothermal approach using ammonium salt of both transition metal, NH_4VO_3 and $(NH_4)_6Mo_7O_{24}$ $4H_2O$ leading to the presence of V^{5+}/V^{4+} and Mo^{6+}/Mo^{4+} oxidation state studied by XPS (Figure 7). The intercalation of Mo^{6+}/Mo^{4+} is found to enhance the electrochemical response when used as cathode in a AZIBs due to the additional redox reactions involving $Mo^{4+}/Mo^{5+}/Mo^{6+}$, to promote the diffusion due to an expanded layer spacing as well as to stabilize the capacity upon insertion and de-insertion of hydrated Zn^{2+} cation cycling.

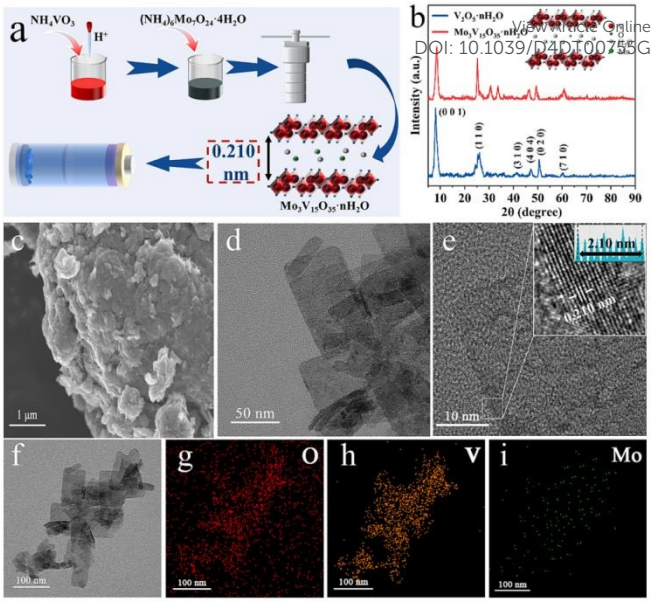

Fig. 7 a) Diagram illustration of the sample preparation of $Mo_3V_{15}O_{35}{\cdot}nH_2O$. b) XRD patterns of $V_2O_5{\cdot}nH_2O$ and $Mo_3V_{15}O_{35}{\cdot}nH_2O$. c) SEM image, d-e) TEM and HRTEM images, and f-i) TEM elemental mapping images of $Mo_3V_{15}O_{35}{\cdot}nH_2O$. Reproduced with permission from ref. 148. Copyright (2024) Elsevier.

Bi-(multi) phasic compounds exhibit phase boundaries of interest for interfacial adsorption-insertion mechanism as predicted and experimentally observed for a biphasic vanadate in aqueous medium with the adsorption and insertion of $Zn^{2+}$and H^+ leading to stable cycling capacities.[145]As an example, the modification of zinc anodes using a ball-milling clay containing $Ti_3C_2T_x$ to build a three-dimensional (3D) framework on the surface of zinc foil was reported by Li et al..[149] One interesting feature in this process is that electrostatic adsorption of functional groups increases the transport dynamics of Zn^{2+} ions, while the 2D diffusion of Zn^{2+} ions in the plane is constrained by the confinement effect of $Ti_3C_2T_x$, which uniformly nucleates Zn^{2+} ions and restricts dendrite growth. A stable long cycle is achieved (2000 h, 0.5 $mAh.cm^{-2}$) in this case. One additional interest of this preparative method stands in the protecting effect of the ball milling clay toward zinc self-corrosion and electrochemical corrosion in the electrolytes. LDHs nanosheets decorating onto carbon improve the energy efficiency of an alkaline zinc-iron flow battery due to the presence of mesoporous texture. This is coming from the hydroxyls covered LDH platelets grown in situ that make the adsorption and ion mass transport easier for the zinc-based battery.[150] Another article reports the use of glucose pillared Ni-Co LDH as a cathode material providing a high specific capacity and stability upon cycling for alkaline zinc batteries.[151] In order to suppress the dendrite growth at the Zn anode, a chitosan gel is coated on its surface while a partially sulfidated NiCoFe LDH platelets that are efficiently exfoliated are combined with reduced graphite oxide to be used a cathode, resulting in an outstanding specific power.[152] Interestingly, sulfur mismatch substitution of NiFe LDH when deposited on nitrogen-doped graphene leads to an electron

transfer between the sulfur anion and Fe^{3+} producing Fe^{4+} species, having as an effect to reach high power and energy density for a Zn-air battery associated with a long cycle stability.[153] LDH crystalline structure presenting metal-sulfur (especially the Cu-S) bonds by a subtle modulation of the copper and sulfur interaction leads to large specific capacity performed in a zinc battery.[154]

Reversible Mg batteries (RMBs) are evaluated since they may provide high volumetric capacity and in absence of dendrite at the metal anode. The limitation of this technology is to find open structures that are sufficiently efficient and stable against the insertion of Mg^{2+} ion.[155] The article reviews the most representative 1D, 2D and 3D intercalation compounds. Another article compares the multivalent-ion batteries based on Mg^{2+}, Zn^{2+}, and Ca^{2+} ions intercalated in a disordered bi-dimensional compound, and the authors present defective $CaTiO_3$-based perovskite of interest for rechargeable Ca-based batteries.[156]

2.4.c. MIBs (M = Al^{3+}, Fe^{3+}) and Dual

Battery technologies based on highly abundant metals also concerns aluminium (third most available element in the Earth's crust), using Al-based ionic liquid as electrolyte. Among the ongoing research, one of the most challenging in terms of electrode materials concern the AIBs (aluminium-ion energy storage) and CIBs (chlorine-ion battery) in term of cathode and anode electrode materials since the pristine material should accommodate the insertion and desertion of the ion, Al^{3+} and Cl^-, respectively, while keeping stable upon cycling and providing enough conductivity for the diffusion process.

This is nicely exemplified by the use of α-MoO_3 as cathode in AIBs in the air-stable $Al(ClO_4)_3$. $9H_2O$/succinonitrile hydrated eutectic electrolyte (ASHEE) system.[157] The layered structure is found to be stable upon cycling and in situ combination of XAS and XRD demonstrate an average valence state between Mo^{6+} and Mo^{4+}/Mo^{5+} associated to a smooth variation of the local bond distance.

The insertion of the trivalent ions Al^{3+} in an AIB is also presented in a cation-deficient anatase TiO_2 where the vacant sites are used for intercalation.[158]

Intercalation occurs in graphite used as cathodic host material and $AlCl_4^-$ ion as intercalated species, involving acceptor-type GIC. As intercalated/deintercalated species into the graphitic cathode are different from those involved in the simultaneous anodic process (deposition of Al atoms/ions from the Al-foil), there is no more "rocking-chair" mechanism in such a technology. It implies the formulation of very specific ionic liquid electrolytes with the drawback of corrosion phenomena versus materials.[159]

The intercalation of Al^{3+} in an Al battery is also reported with graphite as the cathode and $AlCl_3$/urea as cheap ionic liquid electrolyte.[160] Second stage GIC is observed in charge and high coulombic efficiency and cycling stability are recorded at high current density.

Carbon electrodes are reviewed based on graphite intercalation compounds (GIC) for ion batteries.[161] An additional review focus on theoretical calculations to better understand their band structure, and structural change and stability against Li ions diffusion.[162] A critical issue reports for carbon-based materials and composites in KIBs in non-aqueous electrolyte.[163] Another study reports that graphite does not perform while soft carbon appears to be of interest upon cycling.[164]

Another study reports the interest to insert chloride anions into Fe-based LDH to produce some kind of green rust that helps to convert electrochemically $Fe(OH)_2$ in FeOOH as tested in rechargeable alkaline iron batteries.[165] Such iron redox improves the cycling stability as characterised by a combination of characterizations including operando X-ray diffraction as well as molecular dynamics simulations. Through the phase evolution identified by XRD (Figure 8), such elegant redox system involves some kind of cascade reduction such as:

$Fe(OH)_2 + OH^- \rightarrow FeOOH + H_2O + e^-$

$3Fe(OH)_2 + Cl^- \rightarrow [Fe^{2+}{}_2Fe^{3+}(HO^-)_6]^+[Cl]^- + e^-$

$[Fe^{2+}{}_2Fe^{3+}(OH)_6]^+[Cl]^- + 3OH^- \rightarrow 3FeOOH + Cl^- + 3H_2O + 3e^-$

Indeed, the green rust intermediate avoids the direct reaction predicted by Pourbaix diagrams:

$3Fe(OH)_2 + 2OH^- \rightarrow Fe_3O_4 + 4H_2O + 2e^-$

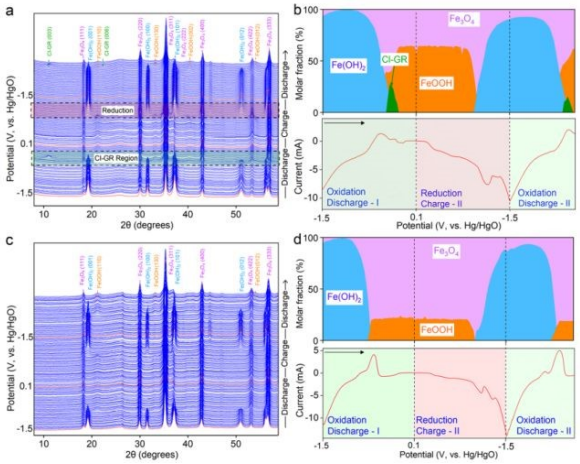

Fig. 8 (a, c) Complete waterfall plots and (b, d) phase ratio analyses of iron oxides in (a, b) NaOH/NaCl and (c, d) NaOH electrolytes using *operando* XRD measurements along with cyclic voltammetry at the scan rate of 0.5 mV/s. The selected regions in (a) show the phase transitions during the Cl− insertion (discharge) and $Fe(OH)_2$ formation (charge). They highlight the XRD patterns depicting the Cl-GR formation when iron oxides were discharged from −0.42 to −0.18 V and the $Fe(OH)_2$ formation when iron oxides were charged from −1.02 to −1.5 V, respectively. The X-ray wavelength is corrected to Cu K_α source (λ = 0.15406 nm). Arrows in (b) and (d) point to the voltage scan direction. Reproduced with permission from ref. 165. Copyright (2023) American Chemical Society.

Dual-ion batteries (DIBs), an emerging energy storage system, use the properties of graphite to insert both anions and cations thus to act as a unique material associated to the electrochemical redox reactions at both electrodes.[166] The two recent reviews cover the

advantages (high energy density, low cost) and disadvantages (cycling stability, electrolyte decomposition) of the DIBs operating at working potential over 4.5 V *vs*. Li/Li^+ as well as some promising strategies.

The modification of the interlayer distance between graphene planes is also a way to explore in order to improve intercalation, especially for sodium-ion batteries. Except alkali metal ion GIC, other covalent or ionic intercalation compounds can be envisaged in order to develop battery technologies such as fluorinated graphite, $FeCl_3$-GIC, anion intercalated graphite. The possibility to develop high voltage dual ion battery with both the formation of cationic GIC and anionic GIC as anode and cathode respectively is also under development. The use of advanced electrolytes including ionic liquids is necessary a subsequent development in order to withstand the operating voltage.[167,168]

2.4.d. Halide ion batteries and other merging systems

New nano and micro-structuring of materials aim to optimise the combination of solid-state electrolytes (SSEs) and electrode materials, particularly focusing on their ionic pathways at interfaces. Hybrid solid polymer electrolytes containing clays as inorganic fillers have emerged as a promising solution, as reviewed recently.[169,170] Clays enhance the ionic conductivity of polymer electrolytes[171] and improve their mechanical and electrochemical properties. Furthermore, incorporating clays in the polymer matrix reduces crystallinity, acts as a solid softener, and enhances compatibility with Li electrodes, ensuring stable cycle performance.[172] To address the hydrophilic nature of clays, which can be incompatible with hydrophobic polymers, methods such as ion exchange or organic moiety grafting are employed to reduce their surface energy. Depending on the preparative techniques, clays can be exfoliated, intercalated, or preserved with a cohesive layer structure within the polymer background. The structure of clay-polymer composites significantly influences conductivity, with exfoliated clay minerals exhibiting the highest ionic conductivity due to increased layer dissociation and specific surface area.[173]However, attention must be paid to the clay content, as excessive loading can lead to aggregation, promoting polymer crystallinity and hindering ion mobility.[170] In the realm of sodium-ion batteries (NBIs), an innovative approach was proposed to develop sodium-ion nano-ionic hybrid solid electrolytes by infusing ceramic halloysite-based Na_2ZnSiO_4 (NZS) with an ionic liquid solution and sodium trifluoromethanesulfonimide (NaTFSI salt), the authors aimed at modify the grain-grain interface of Clay-NZS, thereby reducing grain boundary resistance and enhancing sodium cation transport properties.[174] This hybrid solid electrolyte exhibited promising potential for application in rechargeable sodium-ion batteries. Because low volume expansion all-solid-state fluoride-ion batteries (FIBs) that use fluoride ions as carrier ions such as for K_2NiF_4 obtained from topochemical substitutive fluorination reactions of Sr_2TiO_4 to $Sr_2TiO_3F_2$ followed by its reductive defluorination/hydride-fluoride-substitution studied by neutron powder diffraction.[175] Interestingly, DFT based calculations of formation energies show the better reactivity of oxyfluorides compared to oxides underlining the driving force of NaF in the exergonic reductions/hydride-fluoride substitution reactions as compared to the endergonic formation of Na_2O for pure oxide compounds.

In the same vein of « small change may have big effect», the interlayered distance of a Ruddlesden-Popper perovskite oxide, $La_{1.2}Sr_{1.8}Mn_2O_7$, known to be suitable for fluoride-ions intercalation/deintercalation reactions has been optimized as a function of the substitution x in $La_{2-2x}Sr_{1+2x}Mn_2O_7$.[176] The authors found an optimized expansion of the interlayer distance x = 0.35, that corresponds also to the composition in the series presenting the highest capacity and rate performance as cathode in FIBs. The authors explain the good performance under high regime by the fact that a larger spacing suppresses the coulombic repulsion between fluoride-ions and oxide ions.

Other halide-ion batteries are also studied as possible post-lithium technology. Chloride-ion batteries (CIB) using LDHs as cathode are also reported.[177] Computational screening gives some insight of optimized cation LDH composition for the anion insertion electrochemistry. This family of compound is also studied for flexible supercapacitors and alkali metal (Li, Na, K) ion batteries.[178] CoFe LDHs crosslinked with carbon nanotubes (CNT) are studied as an anode in an aqueous CIB.[179] The redox reaction is based on the valence changes of the transition metals and both LDH cations contribute to the capacity by repetitive oxidation and reduction redox reactions through a topochemical mechanism occurring within the platelets while CNTs supply the electronic conductivity. This opens possible application in aqueous desalination technology. Another article reports a usual Ni_5Ti-Cl LDH composition for CIB, giving rise to an efficient retention of the reversible capacity upon cycling.[180]

Another family of layered structure is considered to fulfil the requirement as stable anode material in CIB: layered perovskite oxychlorides A_2TMO_3Cl with A, a strong alkaline metal that may interact with Cl^- ions and T, a transition metal for the redox reaction.[181] The authors select (A,T) = (Ca, Co) and (Ba, Rh) as these compounds maintain their layered structure during the Cl^- (de)intercalation reaction process.

Another forefront research in new energy technology concerns rechargeable aqueous batteries based on ammonium ions. A proof of concept is carried out from a rocking-chair battery using 3,4,9,10-perylenetetracarboxylic di-imide at the anode and Mn_nAl (n = 2 or 3) based LDH as cathode.[182] The full battery was found to deliver an energy density as high as 45.8 $Wh.kg^{-1}$ that was mostly explained by a rapid amorphization of the LDH framework thus helping for the NH^{4+} ion mass transport and storage.

2.5. High power batteries and supercapacitors

On the border between efficient energy density and power density, rapid battery-like intercalation may find place, the so-called pseudocapacitive storage that should be described by capacitance in

mAh/g rather than F/g since it comes from the response of rapid redox active sites and not to surface process only. In that field, layered structures have attracted major attention such as all type of 2D framework possessing redox sites, as long as the latter are well exposed due to large surface area of the high aspect ratio platelets and/or to the presence of highly diffusive pathways thus connecting most of the active mass of the open structure.[183] Only few materials may compete with layered structure: metal oxide framework (MOF) with very large tunnel-based structure at the condition that the connectivity between transition metals and their ligands is stable during the rapid redox reaction.

High A recent article reports hybrid LDHs as materials at both electrodes in an aqueous battery-type device.[184]The feasibility is demonstrated using two electroactive species interleaved into LDH host structure: riboflavin phosphate on one side (negative electrode) and ferrocene carboxylate (FCm) (positive electrode) and then placed face to face. In this set-up, the complete cell cycles up to 2.2 V *vs* Ag/AgCl in sodium acetate aqueous electrolyte.

A controlled morphology is known to be of importance to improve the electrochemical performance as exemplified by copper hydroxide nitrate nanostructures.[185] This is exemplified using simple hydrolysis of salt and oxide or precipitation with alkaline solution, ultrasonication, microwave, urea method in temperature or under reflux. In the figure 4, the crystal aspect ratio L_z/L_{xy} reporting the thickness to lateral size reflects the extent of the structural coherence length along the stacking direction (L_z) and in the plane of the hydroxide layers (L_{xy}), respectively. Such shape anisotropy may be controlled by the chemical preparation and it is found that the different crystalline domains, i.e., $L_z/L_{xy} < 1$ for platelets-like shape or $L_z/L_{xy} > 1$ for rodlike particles thus forming a landscape that can be divided into three large zones (Figure 9), affect the electrochemical activity. In terms of electrochemical activity, some nanostructured submicron particles exhibit a capacity up to 197 mAh.g^{-1}, corresponding to nearly 90% of the theoretical capacity for a two-electron redox process.

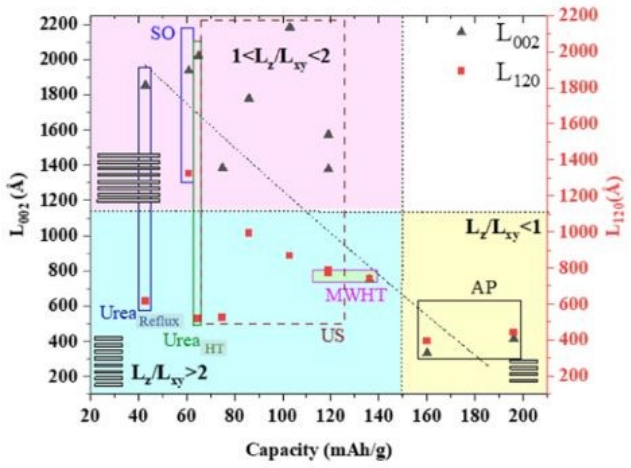

Fig. 9 Correlation between the capacities obtained from the CV of the first cycle and structural coherence lengths L_z and $/L_{xy}$ obtained from XRD analysis for $Cu_2(OH)_3(NO_3)$ samples series with US: ultra-sonification, AP: alkaline precipitation, MWHT: microwave high-temperature, SO: salt and oxide method. Reproduced with permission from ref. 185. Copyright (2023) American Chemical Society.

In the same vein, a similar intercalation compound of copper sulfide[184] is used as both positive and negative electrode material in a complete aqueous battery system but whose performance remains to be optimised.[186] Interestingly in terms of solid-state kinetic approach, copper sulfide is prepared by a pseudomorphic transformation from layered copper hydroxide salt (LSH) ($Cu_2(OH)_3NO_3$) precursor using amine digestion or microwave process. The activation energy to convert LSH into CuS is highly dependent of the process of transformation while a more open-structure (larger anions inside the interlayer LSH) is found to increase the term of entropy, thus more prompt to react and to be transformed into CuS.

It is well known that energy and power are the keys to electrochemical storage systems. After these preliminary studies of power batteries using aqueous electrolyte electrode materials, other systems provide even more power but often at the expense of energy (unless there is rapid redox reaction but then these are power batteries as previously): these are often named supercapacitors, however the mechanism is still based on redox rapid reactions. As mentioned above, the capacitance is often reported in F/g but as it should be expressed in mA.h/g since it is a faradaic process involving a rapid electron transfer and not strictly a capacitive process related to the adsorption of mobile ions in the diffuse layer.

Limited by scarcity of the chemical element as Ir or Ru, some model materials considered as super-capacitor electrodes are abandoned in favour of ILCs. For instance, but rather counterintuitively, acetate inserted into a NiCo-based LDH open structure leads to a reduced interlayer spacing that is found to enhance the structural stability while providing high specific capacitance at high current density.[187] Scrutinized by AC impedance, the intercalation of acetate anions is found to lower the internal electrode material resistance, thus improving the rate performance by a better ion conductivity. When placed as positive electrode and assembled in an asymmetric supercapacitor, the cycling is found to be stable (Table 1).

In the same LDH cation composition but electrodeposited, the intercalation of PO_4^{3-} is found to increase significantly the access and the quantity of the active redox sites.[188] The hybrid composite when used as cathode in asymmetric supercapacitor shows exceptional cycle stability.

Other ILCs are reported such as layered metal chalcogenide nanocrystals[189] or $Ti_3C_2T_x$ MXene structure when intercalated by ethylenediamine (EDA)[190] or assembled with polymer.[191] EDA-$Ti_3C_2T_x$ intercalation compound mostly mesoporous exhibits low charge transfer resistances in H_2SO_4 aqueous electrolytes associated to a large specific capacitance with good retention upon cycling. In

$Ti_3C_2T_x$/PEDOT: PSS hybrid film, PEDOT polymer chains are pillaring MXene flakes to avoid them to aggregate or to self-restack as well as to act as a conductive bridge accelerating the electrochemical reaction through multidimensional electronic transport channels. The outstanding volumetric power density of the films is of interest for flexible and wearable electronic devices.[190] When mixed with LDH, MXenes exhibit high capacity as electrode materials for supercapacitor.[192]

In high-power-ion hybrid Na-ion full cell capacitors, an MXene Ti_2C negative electrode associated to an alluaudite $Na_2Fe_2(SO_4)_3$ as positive electrode delivers a relatively high voltage of 2.4 V associated to 90 mAh.g^{-1} at 1.0 A.g^{-1} (based on the weight of the negative electrode).[193]

Attention was also paid to clays having different structures such as nanotubes (halloysite) and 2D nanosheets (montmorillonite) as candidates for applications as electrode materials for supercapacitors.[194,195,196,197,198] However, montmorillonites face limitations due to their low electronic conductivity and high electrical resistance.[199] Halloysite, with its unique tubular structure, shows promise by providing channels for electrolyte ions, thereby enhancing specific capacitance.[199,200] Yet, it suffers from low conductivity and a small active specific surface.[201] Acid activation emerges as a suitable method to address these weaknesses by increasing active sites, specific surface area, and porosity through inner-wall dissolution.[202]

Various strategies have been proposed to address the issue of low conductivity in clay-based materials. This includes the formation of composites starting from conductive polymers such as polyaniline (PANI) [203] combinations of montmorillonite or halloysite with carbon-based materials like porous carbon, carbon multiwall nanotubes, and reduced graphene oxide.[197] Montmorillonite has also been used as a template for the growth of nickel telluride nanostructures[204] and cobalt boride@clay mineral hybrid composites have been developed. [205] Furthermore, layer assemblies of NiMnLDHs and/or poly(3,4-ethylenedioxythiophene) (PEDOT) onto perforated halloysite nanotubes templates have been achieved through growth and polymerization method. [206] A relevant approach involves forming core-shell heterostructures with hydrangea shapes using LDH@polypyrrole as mirror materials concerning clay minerals for high-performance hybrid supercapacitors. [207]

The investigating of the electrochemical properties of halloysite-polyaniline (PANI) composites formed via in situ polymerization of aniline demonstrated that those prepared from halloysite etched with hydrochloric acid at 0°C exhibited the highest specific capacitance of about 710 F.g^{-1} at a current density of 1 A.g^{-1}, with good cycling stability retaining around 77% of specific capacitance after 300 charge-discharge cycles. [208] MMT/PANI/Co_3O_4 prepared through a two-step process, enables achieving a specific capacitance of 234 F.g^{-1} with a capacitance retention of approximately 97% after 1000 cycles.[203] Clay-conducting poly-o-Toluidine hybrid nanocomposites are also promising compounds for supercapacitor applications. [209]

Combining clays and carbon-based materials is also widely use in order to improve the poor conductiviy of montmorillonite and halloysite. As an example, montmorillonite reduced graphite oxide (rGO) nanocomposites have high specific capacitance and high cycle stability.[210] Using a non-liquid crystal spinning method followed by chemical reduction to produce rGO/clay fibers it is possible to achieve high conductivity and capacitance. [211] A comparison between Polypyrrole-coated carbon nanotubes and Cloisite 30B®/ Polypyrrole-carbon nanotubes composites demonstrated that the addition of Cloisite 30B® led to enhanced electro-active surface and higher specific capacitance.[212] rGO/montmorillonite/Polyvinylcarbazole (PVK) nanocomposites increased specific capacitance compared to pristine rGO/ Polyvinylcarbazole was attributed to the dopant effect of montmorillonite and PVK. [213]The inhibitory effect of montmorillonite nanosheets on the restacking of graphene sheets as well and enhancement of the electrochemical performance were also proven for 3D reduced graphene oxide/montmorillonite aerogels. [214] A robust strategy to form halloysite/carbon composites starting from halloysite and formaldehyde-free phenol-furfural resin synthesised from phenol and sugar-based furfural was also proposed. [215] The challenge to face being finding the best condition enabling to offset the poor conductivity of halloysite with carbon renewable precursor having a higher biomass content. Halloysite was also used in order to meet the demand for flexible and wearable supercapacitors, in this frame, a novel chemical crosslinking of cellulose/ionic liquid/halloysite nanotubes dispersions was formed. [216] Nacre-inspired HPA-rGO nanocomposite films having a high electrical conductivity as well as higher specific capacitance compared with other graphene-based films have been successfully prepared. [217] N-doped graphene quantum dots deposited on Fe_3O_4 -halloysites were also formed[218] the synergetic effects of different compounds enabling the formation of highly performant materials: Fe_3O_4 increase the energy density, Fe_3O_4-HNTs enables to shorten the diffusion path of electrons and electrolyte ions to graphene quantum dots as well as to absorb the mechanical stress during cycling along with excess sites for charge storage. A novel hybrid material based on halloysite, $NiCo_2S_4$ (NCS), and carbon, achieving a maximum specific capacity of 544 mAh.g^{-1} at a scan rate of 5 mV mAh.g^{-1} was also mentioned. [219] In the field of CeO_2-clay it was concluded that the high capacitance is mainly attributed to the increase in specific surface area and improved wettability, with the unique interlayer structure of clay minerals contributing to cycle stability A Comparisons with the literature data for various composites suggest that the performance of CeO_2-clay composites is superior, highlighting the potential of this approach.[220]

2.6. Use in dye-sensitized solar cells (DSSCs)

In the field of energy, clays can also serve as nanofillers for dye-sensitised solar cells (DSSCs now also known as Gratzel cells) electrolytes as recently reviewed. [221, 222, 223] The electrolytes in DSSCs

are responsible, not only for the regeneration of the dye impregnated on mesoporous TiO_2, but also for charge transport between the photoanode and the counter electrode (CE) of the solar cell. [222] Attempts to replace liquid and gel electrolytes were governed by different facts such as their lack of stability during time at the required temperature owing to the leakage and/or evaporation of the organic solvent leading to the need of hermetic sealing. To overcome these problems, polymer-based electrolyte has been introduced for DSSC applications but although their advantages over liquid or gel electrolytes, their power conversion efficiency are lower than those of liquid and gel-based electrolytes as the ionic movements are hindered by the polymeric matrices.

Using nanofillers as multi-functional additives and especially clays is one way to solve this problem and clays play key roles in the properties of electrolytes as well as performance of DSSCs.

2D-materials are found to exceed 3D-materials when pre-intercalation of guest species is needed to assure a structural stability and/or provide an additional property such as water repellence of interest when the materials are used in solar cells. This is nicely illustrated by the 2D perovskite analogues used in solar cells so called perovskite solar cells (PSCs). Using a hydrophobic organic bifunctional spacer with 1,4-phenylenedimethanammonium (PDMA) containing Dion–Jacobson 2D perovskite material $(PDMA)FA_2Pb_3I_{10}$. [224] (Figure 10) The hybrid layered materials when assembled in a solar cell and exposed to humidity is found to be moisture resistant without noticeable degradation and presenting a suitable efficiency of 7%. Similarly, diammonium cations are intercalated in PbI_2 layered structure involved in a 2D/3D perovskite heterojunction. [225] The intercalation helps to orientate 2D nanoplate acting as a template during the growth of the perovskite layer. It is also observed a reduction of defects, a better carrier extraction altogether leading to an efficient power conversion efficiency and making the authors to conclude that the pre-intercalation strategy is appealing for both efficiency and stability challenges in PSCs.

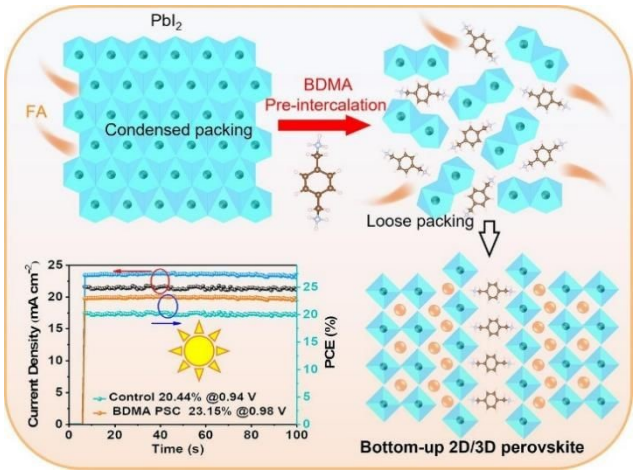

Fig. 10 Perovskite films with BDMA pre-intercalation and photovoltaic performance of PSCs with the steady-state efficiency under continuous illumination at the maximum power point for the control and BDMA PSC. Reproduced with permission from ref. 225. Copyright (2024) Elsevier.

Thanks to their beneficial properties, clays have been widely used as nanofillers for electrolytes in dye-sensitised solar cells (DSSCs). [226] Non-modified clays like saponite and Laponite®, as well as grafted and organically modified clays such as montmorillonite and talc, have been utilised. [227, 228, 229,230] These clays are incorporated into various polymers or polymer mixtures, such as poly(n-isopropyl acrylamide) (PNIPAAm) and iodide poly(vinylidene fluoride-co-hexafluoropropylene) (PVDF-HFP), using conventional methods like in situ polymerization or solution/melt intercalation.[192,194] For instance, the addition of 5 wt% montmorillonite to PVDF-HFP electrolyte significantly improved diffusivity, conductivity, and power conversion efficiency in DSSCs. [231] The coupling of substituted Zn-porphyrins with PMMA and nanoclay-based gel electrolytes in DSSC devices enables achieving a PCE of around 1.55%.[232]This innovative approach demonstrates potential for the development of stable and efficient gel-state electrolytes for DSSCs.

2.6. Hydrogen storage layered materials

The quest for efficient and sustainable hydrogen storage materials has led to exploration into various options, including clay minerals. [233] One solution is underground hydrogen storage[234] where clays, being ubiquitous secondary minerals in natural underground settings, play a significant role. Studies have delved into the contribution of clays in geochemical and reaction path modeling of hydrogen storage in sedimentary rocks. [235] Additionally, research has focused on the wettability of clay surfaces by hydrogen in the presence of brine, which influences injectivities, withdrawal rates, storage capacity, and containment security.[236] Recent investigations have explored the impact of pore structure parameters on hydrogen adsorption under different conditions, revealing that specific surface area and micropore volume positively affect hydrogen adsorption, while average pore width has a negative effect. [237]

Several studies have focused on solid-state hydrogen storage for electrochemical applications, where montmorillonite has shown promise. Modification techniques such as acid-activation, ion-exchange, and grafting have been explored to enhance hydrogen adsorption capabilities. [238, 239] For instance, Metal-Organo-Clays (MOC), synthesised by in-situ formation of metal nanoparticles in montmorillonite-supported polyol dendrimers, have demonstrated improved hydrogen affinity.[240] Copper-loaded organo-montmorillonite were prepared, showing enhanced hydrogen affinity due to reduced nanoparticle mobility and aggregation, favoring physical condensation of hydrogen. [241] $Ca_2Mn_3O_8/CaMn_3O_6$/montmorillonite composites, achieving increased hydrogen storage capacity attributed to spillover, redox, and physisorption mechanisms are also good candidates. [242] Halloysite has also been explored for hydrogen storage, with acid-treated halloysite and hexagonal boron nitride composites exhibiting enhanced hydrogen storage capacity due to increased adsorption sites. [243] Additionally, a composite electrode based on halloysite nanotube-$Li_{0.9}Ni_{0.5}Co_{0.5}O_{2-x}/LiFeO_2$ nanostructures showed higher electrochemical hydrogen storage. [244] The optimization of the key parameters governing the composites formation has led to hydrogen

storage capacities six times higher than pristine halloysite capacity. Clay minerals have been integrated into carbon-based materials to develop clay-carbon composites for hydrogen storage. Combining clay minerals with carbon materials like activated carbon, graphene, or carbon nanotubes has shown potential for enhancing hydrogen adsorption capabilities. [245, 246]

Despite progress, challenges remain, including developing scalable synthesis methods, exploring new composite formulations, and assessing the practical feasibility of clay-based hydrogen storage systems.

2.7. Magnetism/Optoelectronics/Tool of characterization (equipment, analytical…)

In nanoelectronics, intercalation into graphene (*i.e.* intercalation of species between a monoatomic graphene layer and its substrate) is an efficient functionalization method to significantly modify the band structure of graphene. Numerous studied elements have been already checked versus epitaxial graphene obtained by CVT or SiC evaporation. Attention has been paid to alkali and alkaline-earth lanthanide metals, some transition metals or even noble metals like gold, and a recent review can be retrieved. [247] These authors also present an original experimental study interested in intercalation mechanism, electronic properties and superconductivity. By a deposition-annealing two-steps process, electronic decorrelation of graphene from its growth substrate is possible, exacerbating its electronic properties and modifying the band structure. Depending on the nature of the metallic element, two different intercalation mechanisms are proposed. For elements with low affinity versus graphite (d-block metals for instance), a diffusion mechanism through graphene defects is evidenced, with the intercalated species located between buffer layer and true graphene. Considering s-block or f-block elements whose affinity versus graphite is higher, a possible diffusion through carbon layer is proposed.

Since the discovery of superconducting properties in CaC_6 with a critical temperature of 11.5K,[248] the highest for this class of materials, the physical properties of donor-type GIC have been deeply (re)investigated. Especially, interest has been focused on alkaline-earth-based GIC and the nature of the superconductivity is commonly explained by BCS theory and electron-phonon coupling that can be easily studied with such materials. If beryllium has still not been intercalated into graphite, successful bulk intercalation reactions have been performed with Ca, Sr and even Ba.[249] In this later case, the increase of the interlayer distance together with the decrease of the charge transfer upon intercalation lead to a very low Tc of only 65 mK.[249]

In order to understand the superconducting properties of intercalated graphite, it is interesting to focus on the nanoscale. As claimed before, intercalation into graphene (one-atomic-layer-honeycomb-network) is impossible but the experimental study intercalated bilayer of few-layers graphene can be realised and brings information on the evolution of coupling versus dimensionality.[250]

Superconducting properties can also be tuned at the nanoscale by twisting, heterostructure elaboration or interlayer separation control in order to control the electronic.[251]

Optimised synthesis of misfit compound containing BiSe, Bi_2Se_3, and $MoSe_2$ constituent layers leads to the formation of $(BiSe)_{0.97}(Bi_2Se_3)_{1.26}(BiSe)_{0.97}(MoSe_2)$ containing metallic 1T-$MoSe_2$, showing charge transfer and a low resistivity with a metallic temperature dependence.[252] Upon Cu topological intercalation into the parent insulator heterostructure compound $(PbSe)_5(Bi_2Se_3)_6$, a superconducting state is reached for $Cu_x(PbSe)_5(Bi_2Se_3)_6$ (CPSBS with $x = 1.47$).[253]

Another heterostructure based on $Bi_2S_3/AgBiS_2$ prepared by a cation exchange reaction from the binary parent compound Bi_2S_3 shows high light absorption coefficient for the enhancement of the photoinduced properties.[254]

A two-dimensional transition metal nitride Ti_2N (MXene) obtained from selective etching of Al from ternary layered transition metal nitride Ti_2AlN exhibits a Surface enhanced Raman scattering (SERS) activity.[255]

Intercalation chemistry combined with exfoliation is known to be a versatile strategy to modulate heterostructure and their electronic structure. This is exemplified with δ-$Sr_{0.50}V_2O_5$ and its intercalation-driven exfoliation to 2D nanosheets.[256]

Concerning tools of characterization of intercalated graphite and carbon-based materials, numerous *operando* techniques (Diffraction, microscopy, spectroscopy [257] are developed in order to understand the behaviour upon alkali ion intercalation in corresponding technology)[258], NIB [259] and KIB.[260,261]

A diacetylene monomer layered crystal structure hosting organic amines through intercalation is found to polymerize leading to polydiacetylene with amine, the whole presenting some tunable stimuli (mechano)-responsive colour-change properties.[262] The colour change is tuned from the nature of the intercalated amines.

3. Summary of the latest developments

To compare the performance of layered structure between each other in terms of capacity and its associated retention in time, voltage window, polarization and hysteresis, energy and power densities, it is usually a difficult task since the experimental condition including the mass of active material, the relative amount of electronic carbon black, nature of the electrolyte and salt, cycling regime may be different between studies. For that reason, a selection of the most recent articles is given in table 1 reporting the best performances for some lamellar materials to streamline «beyond Li» future technologies. Energy and power densities are not reported since the data in the literature are not complete and refer often to complete electrochemical devices making difficult comparison for each electrode material.

Table 1. Selected recent articles using layered structure reporting original proof of concept for the possible «beyond LIBs» technology including: sodium-ion (NIB), potassium-ion (KIB), aluminium-ion (AIB), aqueous zinc-ion (AZIB), aqueous chloride-ion (ACIB) battery and supercapacitor (SC) storage system, the layer composition and guest species indicated, the capacity and its retention upon cycling when available in half-cell or full-cell.

ICLs	Guest	Battery or SC	Capacity	Retention (%) (N cycles)	Ref
$TiSe_2$	PA/HA [b]	NIB	417 mA.h/g (@1 A/g)	95 (2,000)	135
$MoSe_2$	Ethylene glycol	NIB	326 mA.h/g (@5 A/g)	87 (200)	134
$MnPS_3$	Me_4N^+	NIB	890 mA.h/g (@0.1 A/g)	94 (700)	132
$KVOPO_4$	K^+	NIB	120 mA.h/g	88 (150)	133
MXene V_2C MXene V_2C	ABS [c] -	KIB (anode) & Dual (SC)	174 mA.h/g 121 mA.h/g (@0.05 A/g)	80 (900) 45 (900)	142
Graphite	Na^+/ether-based molecule	NIB	110 mA.h/g (@0.1 A/g)	>99% (2500)	125
Graphite	K+-solvent	KIB			130
Graphite	-	AIB (cathode) $AlCl_3$:urea	73 mA.h/g (@ 0.1 A/g)		160
(VOH) [a]	Mo^{6+}	AZIB	430 mA.h/g (@ 0.1 A/g)	95 (1,000)	168
Birnessite δ-MnO_2	Na^+, Cu^{2+}	AZIB	576 mA.h/g		147
LDH NiCo	Glucose	Alkaline Zn	224 mA.h/g	86 (2,000)	151
LDH CoFe	Cl^-	ACIB	190 mA.h/g (@ 0.2 A/g)	66 (200)	179
LDH Ni_5Ti	Cl^-	CIB	129 mA.h/g (@ 1 A/g)	100 (1,000)	180
LDH Mn_3Al	CO_3^{2-}	NH_4^+ [f]	184 mA.h/g (@ 0.1 A/g)		182
MXene $Ti_3C_2T_x$ MXene $Ti_3C_2T_x$	EDA [d] PEDOT/PSS [e]	SC (H_2SO_4) SC (H_2SO_4)	486 F/g 1313 (F/cm^3) 1065 F/cm^3	89.7 (10,000)	190 191
LDH NiCo	Acetate	SC	1032 F/g		187
NiCo	PO_4^{3-}	SC	87 mA.h/g 2070 (F/g)	92 (10,000)	188

[a] (VOH) = Hydrated vanadium oxide; [b] PA/HA = Propylamine/hexylamine; [a] ABS = azobenzene sulfonic acid; [d] EDA = =ethylenediamine; [e] PEDOT:PSS = Poly(3,4-ethylenedioxythiophene) polystyrene sulfonate ; [f] NH_4^+ = rechargeable aqueous ammonium-ions battery.

Table 1 summarizes the benefit of 2D materials for some «beyond LIB» electrochemical systems. The possibility in substituting intra-layered redox metal is not unusual as many inorganic compounds present solid solution. However, some 2D compounds present the possibility of having multiple substitutions such as LDH resulting in the presence of diverse redox metal.[263] Such versatile 2D template may be of interest to increase the electronic delocalization, *i.e.* the electronic conductivity to ease the intercalation and deintercalation in some of these «beyond LIB» systems as well as to optimize the energy density, this is available for intercalation but also conversion type mechanisms where the volume change should be minimized. The expansion of the interlayer spacing is of high-value for 2D system since it permits big-size ion to migrate in and out of the structure compared to other rigid open-framework formed by tunnels. Indeed, even a small change in the spacing value may have a lot of effect for long term performance as illustrated by $KVOPO_4$ in NIBs instead of $NaVOPO_4$ [133] or for the solid solution $La_{2-2x}Sr_{1+2x}Mn_2O_7$ tested in FIBs.[176] Evidently this is more pronounced with a large expansion such as observed for acetate in NiCo LDH for SC application[187] and even more when the interleaved species is redox-active such as V_2C MXene pre-intercalated with azobenzene sulfonic acid tested in KIB.[132]

4. Recycling ILCs

Recycling in spent lithium-ion batteries is scarcely reported but should increase to respond to the strong requirement regarding sustainability and life cycle assessment of used materials. In the study,[264] the authors report the fluorination process of spent cathode materials (LCO and NMC) converted to CoF_2 and mixed transition metal fluorides, able to further deliver energy.

A study reports the use of water molecule intercalation to regenerate under mild calcination the de-lithiated cathode material NCM ($LiNi_{0.55}Co_{0.15}Mn_{0.3}O_2$).[265] Such intercalation leads to a phase transformation induced by a lattice expansion along the stacking direction, that is nicely used to form a renewed electrode material after soft hydrothermal treatment. As another perspective, if graphite recycling remains economically of low interest, it also becomes mandatory regarding sustainable policies and recent works in this field are also emerging from the literature.[266, 267, 268, 269]

5. Remarks and outlook

In this essay, we aimed to give some up-to-date insights on ILCs syntheses and the associated elaborate experimental protocol to modify, functionalize, decorate these materials so that they are suitable when mixed with other constituents such as a polymer or compound to form a larger scale architecture and also to give them specific properties. We can distinguish the two main approaches which consist of bottom-up or top-down. The first concerns syntheses in micellar medium, the preference of nucleation over the phenomenon of crystal growth, the second exfoliation as for clays, -ZrP and GIC to give graphene. Other methods make it possible to obtain hybrid materials.

Thus, it is described to clay modification through organo-modification and more specifically in the case of cationic clay organoclay colloidal route. Another interesting treatment is the intercalation-exfoliation reaction (Hummer's based interaction reaction), that is somehow reminiscent of the reductive intercalative polymerization (RIP)[270] or of the topochemical oxidative reaction (TOR).[271]

The use of ICs in the field of electrochemical energy storage gives rise to an abundant literature since ILCs meet almost all the criteria, the first that linked to the diffusion of species, the second linked to their electronic conductivity which can be improved. A recent and summary overview is given on technologies linked to lithium-ion battery (LIB) and those after LiB so called «beyond LIB» such as XIB (X = Na (NIB), K (KIB), Al (AIB), Zn (ZIB), Cl (CIB), Dual-ion batteries (DIB) as well as other possible systems such as reversible Mg batteries (RMB), Zn-air, Zn-sulphur, ILCs feature adaptable compositions that can often accommodate redox centres for electrochemical reactions occurring at potentials conducive to their use as either an anode or cathode of a complete system. The advantages of ILCs for these «beyond LIB» technologies are briefly summarized in Table 2.

Table 2. Conclusive remarks to qualitatively evaluate the advantages of layered structure in electrochemical «beyond LIB» systems, XIB (X= Na^+, K^+, Al^{3+}, Zn^{2+}, Cl^-) and SC.

Intralayer redox metal Substitution	Interlayer Spacing	Interleaved redox Species	Exfoliation & Interstratification
Tune potential discharge and charge Energy density ↗ Hysteresis ↘ Conversion reaction Volume change limitation	Insertion and desertion of large size ions Electrolyte wettability Diffusion ↗ Power density ↗	Pillared 2D stacking No structure collapses Number of cycles ↗ Additional capacity performance Performance ↗	To form composite with other compounds Adaptable response Dual system Energy & Power ↗
XIB and SC mostly concerned:			
All	KIB, AIB, ZIB	KIB, CIB	All

This is very classically illustrated by the positive materials used in LIBs. But also, surprisingly even the least expected ILCs in terms of redox reaction for electrochemical storage systems have been considered or in part to form composite electrode materials. This is the example in particular of clays with conjugated polymers to limit the stress caused by changes in volume under electrochemical grinding or to form templates for carbonization to obtain carbon with a high specific surface area for supercapacitor applications.

Finally, it is obvious that the field of energy for intercalation compounds has witnessed significant advancements and holds great promise for addressing the challenges associated with energy storage. Several perspectives emerge for the future of energy storage based on ILCs:

- the development of new synthesis methods with a focus on the development of sustainable and environmentally friendly solutions (with low CO_2 footprint),

Notes and references

- as these versatile materials are scalable nowadays, to target a high Technology Readiness Level (TRL) avoiding the valley of death which brings down many new proposals resulting from research but to transfer those that are innovative but also pragmatic in economic and sustainable development terms and no longer simple easy alternatives,

- to develop new recycling strategies to minimize the environmental impact of intercalation-based energy storage technologies, and integration of renewable energy sources into the grid as the compounds can help addressing their intermittency.

ILCs may be viewed as chemical toolbox that can tackle critical features for energy storage and future challenges, while also balancing sustainability and scalability in the same time as well as ensuring a greener future. It explains the reason why many ILCs are revisited in the case of «beyond LIB» systems.

We are convinced that ILCs will meet the challenge due to their versatility in terms of chemical composition, structuring, shaping as well as for those being ion exchange materials the possibility to expand their interlayer space to increase the diffusion process, to be organo-modified with active redox guest. The unstacking through exfoliation results in layers*, i.e.*, redox centres, more exposed as well as the possibility of being interstratified when restacked with other layers to form heterostructures or to be simply mixed with other materials to form complex architectures of interest.

Conflicts of interest

There are no conflicts to declare.

Acknowledgements

All co-authors as well as all colleagues from the board of the International Symposium on Intercalation Compounds (ISIC) are warmly acknowledged.

References

1 F. Chang, I. Tezsevin, J.W. de Rijk, J.D. Meeldijk, J.P. Hofmann, S. E.R, P. Ngene, P.E. de Jongh, *Nature Catalysis,* 2022*,* **5**(3), 222-230.

2 S. Cahen, L. Speyer, P.Lagrange, and C. Herold, *Eur. J. Inorg. Chem.,* 2019, **45**, 4798-4806*.*

3. A. Lyo, H. Ogino, S. Ishio and H. Eisaki, *Adv. Mater.,* 2023, **35** (15), e2209964-.

4 A. Lyo, H. Fujihisa, Y. Gotoh, S. Ishida, H. Eisaki, H. Ogino and K. Kawashima, *Carbon,* 2023, **215**,118381-118398.

5 M. Laipan, L. Xiang, J. Yu, B. R. Martin, R. Zhu, J. Zhu, H. He, A. Clearfield and L. Sun, *Prog. Mater. Sci*, 2020, **109**, 100631.

6 C. Xu, M. Zhang,X. Yin, Q. Gao, S.Jiang, J. Cheng, X.Kong, B. Liu, H.-Q. Peng, *J. Mater. Chem. A*, 2023, **11**, 18502–18529.

7 Y.C. Lin, R. Torsi, R. Younas, C.L.Hinkle, A.F.Rigosi, H. M. Hill, K. Zhang, S. Huang, C.E. Shuck,C.Chen, Y. H. Lin, D. Maldonado-Lopez, J.L. Mendoza-Cortes, J. Ferrie, S. Kar, N. Nayir, S. Ragjabpour, A.C.T. Van Duin, X. Liu, D. Jariwala, J. Jang, J. Shi, W. Mortelmans, R. Jaramillo, J. M. J. Lopes, R. Engel-herbert, A. Trofe, T. Ignatova, S. H. Lee, Z. Mao, L. Damian, Y. Wang, J. L. Knappenberger Jr, Z. Wang, S. Law, G. Bepete, Y. Wang, D. Zhou, J.-X. Lin, M. S. Scheurer, J. Li, P. Wang, G. Yu, S. Wu, D. Akinwande, J. M. Redwing, M. Terones, J. A. Robinson, *ACS Nano,* 2023, **17** (11), 9694–9747.

8 Z. Guo, F. Sun and W. Yuan, *Cryst. Growth Des.* 2017, **17**(4), 2238–2253.

9. I. Kassan Belay, T.A. Shifa, S. Zorzi, M.G. Senduku, E. Moretti, , A. Vomiero, *Prog. Mater. Sci.*, 2024, **144,** 101287-101315.

10 A. R. Sotiles, L.M. Baika, M.T. Grassi and F. Wypych, Fernando, *J. Am. Chem. Soc.*, 2019, 41(19)8001-8002

11 Z. Li, X. Zhang, H.Cheng, J. Liu, M.Shao, M; Wei, D.G. Evans, H. Zhang and X. Duan, *Adv. Energy Mater.*, 2020, **10**, 1900486

12 S. Yahya, S. K.M.Wahab and F.W. Harun, *Renew. Energy*, 2020, **157**, 164–172.

13 S. Barakan and V. Aghazadeh, *Environ Sci Pollut Res Int*, 2021, **28**, 2572–2599.

14 H. Han, M.K. Rafiq, T. Zhou, R. Xu, O. Mašek, and X. Li, *J. Hazard. Mater*., 2019, **369**, 780-796.

15 S. Akbulut, Z. Nese Kurt and S. Arasan, *Earth Sci. Res. J.*, 2012, **16**, 95-101.

16 S. Taymouri and J. Varshosaz, Adv. Biomed. Res., 2016, **5.** 48

17 G. Xue, M. Gao, Z. Gu, Z. Luo and Z. Hu, *Chem. Eng. J.,* 2013, **218**, 223–231.

18. R. Wei, Y. Mo ,D. Fu, H. Liu, B. Xu, Molecules 2023, **28**,2021-2037.

19 J.M.Thomas and W.J Thomas, W.J., 2014, Principles and practice of heterogeneous catalysis, John Wiley & Sons, 2014.

20 T. Mishra and D.K. Mahato, *J. Environ. Chem. Eng*., 2016, **4**, 1224–1230.

21 F. Tomul, *Appl. Clay Sci*., 2016, **120**, 121–134.

22 (a) L. Chmielarz, A. Kowalczyk, M. Skoczek, M. Rutkowska, B. Gil, P. Natkański, M. Radko, M. Motak, R. Dębek and J. Ryczkowski*, Appl. Clay Sci.,* 2018, **160**, 116–125.

23 M. Munoz, M. Greber, K.B. Tayed, C. Lamonier, C.I. Carole, *Green Processing & synthesis*,2023, **12**,20230026-20230038. View Article Online DOI: 10.1039/D4DT00755G

24 E. Ruiz-Hitzky, P. Aranda, M. Akkari, N. Khaorapapong and M. Ogawa, *Beilstein J. Nanotechnol.,* 2019, **10**, 1140–1156.

25 R. Ma and T. Sasaki, *Acc. Chem. Res.,* 2015, **48**(1), 136-143.

26 (a) M. Khan, M.N. Tahir, S.F. Adil, H.U. Khan, M.R.H. Siddiqui, A.A. Al-Warthan and W. Tremel, *J. Mater. Chem. A*, 2015, **3**, 18753-18808. (b) M. Yi and Z. Shen, *J. Mater. Chem. A*, 2015, **3**(22), 11700-11715.

27 S.E. Lowe, G.P. Simon and Y.L. Zhong, *Curr. Opin. Colloid Interface Sci.,* 2015, **20**(5-6), 329-338.

28 G. Bepete, F. Hof, K. Huang, K.Kampioti, E. Anglaret, C. Drummond and A. Penicaud, *Phys. Status Solidi - Rapid Res. Lett.*, 2016, **10(**12), 895-899.

29 N.I. Zaaba, K.L. Foo, U. Hashim, S.J. Tan, W.W. Liu and C.H. Voon, *Procedia Eng*., 2017, **184**, 469-477.

30 J. Cao, P. He, M.A. Mohammed,X. Zhao, R.J. Young, B. Derby, I.A. Kinloch and R.A.W. Dryfe, *J. Am. Chem. Soc.*, 2017, **139**(48), 17446-17456.

31.C. Backes, A.M. Abdelkader, C. Alonso, A. Andrieux-Ledier, R. Arenal, J. Azpeitia, N. Balakrishnan, L. Banszerus, J. Barjon, R. Bartali, *2D Mater.*, 2020, **7**, 022001

32 E. Grånäs, T. Gerber, U.A. Schröder, K. Schulte, J.N. Andersen, T. Michel and J. Knudsen, *Surf. Sci*., 2016, **651**, 57-61.

33 Y. Xiao, G. Tian, W. Li, Y. Xie, B. Jiang, C. Tian, D. Zhao and H. F *J. Am. Chem. Soc*., 2019, **141**(6), 2508-2515.

34 W.J. Ong, L.L. Tan, Y.H. Ng, S.T. Yong and S.P. Chai, *Chem. Rev.,* 2016, **116**(12), 7159-7329.

35 N. Mao, C.H. Zhou, D.S. Tong, W.H. Yu and C.X.C. Lin, *Appl. Clay Sci*., 2017, **144,** 60-78.

36 T.T. Zhu, C.H. Zhou, F.B. Kabwe, Q.Q. Wu, C.S. Li, and J.R. Zhang, *Appl. Clay Sci*., 2019, **169**, 48–66.

37 Y. Zhao, F. Li, R. Zhang, D.G. Evans and X. Duan, *Chem. Mater.,* 2002, **14**, 4286-4291.

38 S. Guo, D. G. Evans, D. Li and X. Duan. *AIChE J*., 2009, **55 (**8), 2024-2034.

39 S. Bai, S, T. Li, H. Wang, L. Tan, Y. Zhao and Y. Song, *Chem. Eng. J.,* 2021, **419**, 129390.

40 D. Barman, S. Ghosh, S. Paul, B. Dalal and S. Kumar De, *Chem. Mater.,* 2018, **30**(16), 5550-5560.

41 X. Zhou, B. Wilfong, H. Vivanco, J. Paglione, C. M. Brown and E. E. Rodriguez, *J. Am. Chem. Soc*., 2016, 138(50), 16432-16442.

42 S. Sasaki, D. Driss, E. Grange, J.-Y. Mevellec, M. T. Caldes, C. Guillot-Deudon, S. Cadars, B. Corraze, E. Janod, S. Jobic and L. Cario, *Angew. Chem. Int. Ed.,* 2018, **57**(41), 13618-13623.

43. S. Sasaki, M.T. Caldes, C. Guillot-Deudon, I. Braems, G. Steciuk, L. Palatinus, E. Gautron, G. Frapper, E. Janod, B. Corraze, S. Jobic and L. Cario, *Nat. Commun*., 2021, **12**(1), 3605.

44 Y. Wang, K. Yamamoto, Y. Tsujimoto, T. Matsunaga, D. Zhang, Z. Cao, K. Nakanishi, T. Uchiyama, T. Watanabe, T. Takami, H. Miki, H. Iba, K. Maeda, H. Kageyama and Y. Uchimoto, *Chem. Mater.* 2022, 34, 2, 609–616.

45 K. Wissel, S. Dasgupta, A. Benes, R. Schoch, M. Bauer, R. Witte, A.D. Fortes, E. Erdem, J. Rohrer, and O. Clemens, *J. Mater. Chem. A*, 2018, 6(44), 22013-22026.

46 T.R. Graham, J.Z. Hu, X. Zhang, M. Dembowski, N.R. Jaegers, C. Wan, M. Bowden, A.S. Lipton, A.R. Felmy, S.B. Clark and K.M. Rosso, C.I. Pearce, *Inorg. Chem.,* 2019, **58(**18), 12385-12394.

47 T. Stimpfling, A. Langry, H. Hintze-Bruening and F. Leroux, *J. Colloid Interface Sci*., 2016**, 462**, 260-271.

48 (a) A. Bashir, S. Ahad, L.A. Malik, A. Qureashi, T. Manzoor, G.N. Dar and A.H. Pandith, *Ind. Eng. Chem. Res.*, 2020, 59(52), 22353-22397. (B) M. Pica, A. Donnadio and M. Casciola, *Coord. Chem. Rev.*, 2018, **374**, 218-235. (c) H.P. Xiao and S.H. Liu, *Mater. Des.,* 2018, **155**, 19-35.

49 G. Alberti and E. Torraca, *J. Inorg. Nucl. Chem*., 1968, **30**, 317-318.

50 D. Capitani, M. Casciola and A. Donnadio, R. Vivani, *Inorg. Chem*., 2010, **49**(20), 9409-9415.

51 J.F. Yu, H. Ding, J. Lampron, B.R. Martin, A. Clearfield and L.Y. Sun, *Inorg. Chem.*, 2020, 59(2), 1204-1210.

52 W.J. Mu, Q.H. Yu, R. Zhang, X.L. Li, R. Hu, Y. He, H.Y. Wei, Y. Jian and Y.C. Yang, *J. Mater. Chem. A*, 2017, **5**(46), 24388-24395.

53 S. Bevara, P. Giri, S.J. Patwe, S.N. Achary, R.K. Mishra, A. Kumar, A.K. Sinha, C.P. Kaushi and A.K. Tyagi, *J. Environ. Chem. Eng.,* 2018, **6**(2), 2248-2261.

54 Y. Cheng, X.D. Wang, S. Jaenicke and G.K. Chuah, *ChemSusChem*, 2017, **10**(16), 3235-3242.

55 Y. Cheng, X.D. Wang, S. Jaenicke and K. Chuah, *Inorg. Chem.,* 2018, **57**(8), 4370-4378.

56 Y. Cheng, H.W. Zhang, J.A. Jaenicke, E.C.P. Tan and G.K. Chuah, *ACS Sustain. Chem. Eng.,* 2019, **7**(1), 895-904.

57 (a) U. Ciesla, S. Schacht, G.D. Stucky, K.K. Unger and F. Schuth, *Angew. Chem.-Int. Edit. Engl.* 1996**, *35*** (5), 541-543; (b) J. Jimenez-Jimenez, P. Maireles-Torres, P. Olivera-Pastor, E. Rodriguez-Castellon, A. Jimenez-Lopez, D. J. Jones and J. Roziere, *Advanced Materials* 1998, **10** (10), 812-815.

58 A. Tarafdar, A. B. Panda, N. C. Pradhan and P. Pramanik, *Microporous and Mesoporous Materials*, 2006, **95**(1-3), 360-365.

59 Y. Sun, P. Afanasiev, M. Vrinat and G. Coudurier, *J. Mater. Chem*., 2000, 10(10), 2320-2324.

60 Z. Y. Yuan, T. Z. Ren, A. Azioune, J. J. Pireaux andB. L. Su, *Catal. Today*, 2005, **105**(3-4), 647-654.

61 K. Saravanan, K. S. Park, S. Jeon and J. W. Bae, *ACS Omega*, 2018, **3**(1), 808-820.

62 R. Chakraborty, K. Bhattacharaya and P. Chattopadhyay, *Appl. Radiat. Isot*., 2014, **85**, 34-38.

63 X. Y. Tian, W. He, J. J. Cui, X. D. Zhang, W. J. Zhou, S. P. Yan, X. N. Sun, X. X. Han, S. S. Han and Y. Z. Yue*, J. Colloid Interface Sci.,* 2010, **343**(1), 344-349.

64 G. Alberti, M. Casciola, F. Marmottini and R. Vivani, *J. Porous Mat*., 1999, **6**(4), 299-305.

65 M. V. Ramos-Garces, J. Sanchez, K. La Luz-Rivera, D. E. Del Toro-Pedrosa, T. F. Jaramillo, J. L. Colon, *Dalton Trans.* 2020, **49**(12), 3892-3900.

66 (a) Y. Zhu, K. Kanamori, N. Moitra, K. Kadono, S. Ohi, N. Shimobayashi and K. Nakanishi, *Microporous and Mesoporous Materials*, 2016, **225**, 122-127. (b) Y. Zhu, T. Shimizu, T. Kitajima, K. Morisato, N. Moitra, N. Brun, T. Kiyomura, K. Kanamori, K. Takeda, H. Kurata, M. Tafu and K. Nakanishi, *New J. Chem.,* 2015, **39**(4), 2444-2450.

67 A. R. Hajipour and H. Karimi, *Mater. Lett,* 2014, 116, 356-358.

68. M. Pica, A. Donnadio, D. Capitani, R. Vivani, E. Tronia and M. Casciola, *Inorg. Chem*., 2011, **50**(22), 11623-11630.

79 M. Pica, R. Vivani, A. Donnadio, E. Troni, S. Fop and M. Casciola, *Inorg. Chem*, 2015, **54**(18), 9146-9153.

70 (a) Y. H. Yu, Y. P. Chen, M. X. Zeng and Z. D. Cheng, *Mater. Lett.,* 2016, **163**, 158-161; (b) X. Y. Li, G. D. Ding, B. L. Thompson, L. D. Hao, D. A. Deming, Z. M. Heiden and Q. Zhang, *ACS Appl. Mater. Interface*s, 2020, 12(27), 30670-30679; (c) D. L. Huang, H. F. Xu, B. S. Jacob, R. Ma, S. Yuan, L. C. Zhang, M. S. Mannan and Z. D. Cheng, *J. Loss Prev. Process Ind*., 2020, **66**, 104183.

71 H. Ding, A. Ahmed, K. Y. Shen and L. Y. Sun, *Aggregate*, 2022, e174.

72 (a) G. Alberti, M. Casciola and U. Costantino, *J. Colloid Interface Sci*., 1985, **107**(1), 256-263. (b) R. M. Tindwa, D. K. Ellis, G. Z. Peng

and A. Clearfield, *J. Chem. Soc. Faraday Trans*., 1985, **81**, 545-552. (c) G. Alberti, J. Marmottini, *J. Colloid Interface Sci.,* 1993, **157**, 513-515.

73 F. C. A. Ding, H. Ding, Z. Q. Shen, L. Qian, J. Ouyang, S. S. Zeng, T. A. P. Seery, J. Li, G. Z. Wu, S. E. Chavez, A. T. Smith, L. Liu, Y. Li and L. Y. Sun, *Langmuir*, 2021, **37**(25), 7760-7770.

74 (a) M. Pica, A. Donnadio, V. Bianchi, S. Fop and M. Casciola, *Carbohydr. Polym*., 2013, **97(**1), 210-216. (b) X. Lin, D. Schmelter, S. Imanian and H. Hintze-Bruening, *Sci Rep*, 2019, **9**, 16389- 16404(c) H. W. Huang, M. L. Li, Y. Q. Tian, Y. H. Xie, X. X. Sheng, X. Jian and X. Y. Zhang, "Exfoliation and functionalization of alpha-zirconium phosphate in one pot for waterborne epoxy coatings with enhanced anticorrosion performance," *Prog. Org. Coat*., 2020, **138**, 105390.

75 H. Ding, S. T. Khan, K. N. Aguirre, R. S. Camarda, J. B. Gafney, A. Clearfield and L. Y. Sun, *Inorg. Chem*., 2020, 59(11), 7822-7829.

76 (a) L. Y. Sun, W. J. Boo, H. J. Sue and A. Clearfield, *New J. Chem.,* 2007, **31**(1), 39-43. (b) M. Wong, R. Ishige, K. L. White, P. Li, D. Kim, R. Krishnamoorti, R. Gunther, T. Higuchi, H. J. Jinnai, A. Takahara, R. Nishimura and H. J. Sue, *Nat. Commun*., 2014,**5**, 3589.

77 H. J. Sue, K. T. Gam, N. Bestaoui, N. Spurr and A. Clearfield, *Chem. Mater.*, 2004, **16**(2), 242-249.

78 B. Anasori, M. R. Lukatskaya and Y. Gogotsi, *Nat. Rev. Mater*., 2017, **2**(2), 16098.

79 H. Chen, H. Ma and C. Li, *ACS Nano*, 2021, **15**(10), 15502-15537.

80 P. A. Shinde, A. M. Patil, S. Lee, E. Jung and S. C. J. Jun, *J. Mater. Chem. A,* 2022, **10**(3), 1105-1149.

81 Z. Wu, Z. Yang, C. Jin, Y. Zhao and R. Che, *ACS Appl. Mater. Interfaces*, 2021, **13**(4), 5866-5876.

82 L. Verger, C. Xu, V. Natu, H. M. Cheng, W. Ren and M. W. Barsoum, *Curr. Opin. Solid State Mater. Sci*., 2019, **23**(3), 149-163.

83 K. Li, T. Jiao, R. Xing, G. Zou, Q. Zhao, J. Zhou, L. Zhang and Q. Peng, *Green Energy Environ*., 2018, **3**(2), 147-155.

84 Y.T. He, X.X. Shen and Y.H. Zhang, *ACS Applied Nano Mater*. 2024. Early access open.

85 J.L. Yang, Y. Zhang, Y.Z. Ge, S. Tang, J. Li, H. Zhang, X.D. Shi, Z.T. Wang and X.L. Tian, *Adv. Mater*., 2024, 11141.

86 N. Kawaguchi, K. Shibata and T. Mizoguchi, *ACS Phys. Chem. Au*, 2024, early access.

87 S. Parida, A. Mishra, Q. Yang, A. Dobley, C.B. Carter and A.M. Dongare, *J. Mater. Sci*., 2024, **59**(3), 828-846.

88 J.L. Liang, C.B. Wei, D.X. Huo and H. Li, *J. Energy Storage*, 2024, **85**, 111044.

89 H.L. Li, J.Y. Wang, S. Xu, A.Y. Chen, H.Y. Lu, Y. Jin, S.H. Guo and J. Zhu, *Adv. Mater*., 2024, 3073.
View Article Online
DOI: 10.1039/D4DT00755G
90 F. Li, R. Hu, Z.Y. Huang, S.W. Luo, H. Qiao, J.X. Zhong and X. Qi, *Applied Mater. Today*, 2024, **36**, 102069.

91 B. Yang, A. G. Tamirat, D. Bin, Y. Yao, H. Lu and Y. Xia, *Adv. Funct. Mater*., 2021, **31**(52), 2104543.

92 V. Vijayakumar, M. Ghosh, K. Asokan, S. B. Sukumaran, S. Kurungot, J. Mindemark, D. Brandell, M. Winter and J. R. Nair, *Adv. Energy Mater*., 2023, **13**(15), 202203326.

93 H. Chaudhuri and Y.-S. Yun, *J. Power Sources*, 2023, **564**.

94 D. Larcher and J.M. Tarascon, *Nature Chem.*, 2015, **7**, 19–29.

95 W. Zhao, C. Zhao, H. Wu, L. Li, C. Zhang, *J. Energy Storage*, 2024, **81**, 110409.

96 Y. Liu, H. Shi and Z.S. Wu, *Energy Environ. Sci.*, 2023, **16**, 4834-4871

97 J. Asenbauer, T. Eisenmann, M. Kuenzel, A. Kazzazi, Z. Chen and D. Bresser, Sustainable *Energy Fuels*, 2020, **4(**11), 5387-5416.

98 M. Druee, M. Seyring and M. Rettenmayr, *J. Power Sources*, 2017, **353**, 58-66.

99 H. Onuma, K. Kubota, S. Muratsubaki, W. Ota, M. Shishkin, H. Sato, K. Yamashita, S. Yasuno and S. Komaba, *J. Mater. Chem. A*, 2021, **9**(18), 11187-11200.

100 R. Raccichini, A. Varzi, S. Passerini and B. Scrosati*, Nat. Mater.,* 2015, **14**(3), 271-279.

101 K. Share, A. P. Cohn, R. Carter, B. Rogers and C. L. Pint, *ACS Nano*, 2016, 1**0(**10), 9738-9744.

102 Z. Chen, Q.M. Wang, S. Bai, X. Wang, W.L. Lin and Y.N. Zhang, *J. Colloid Inter. Sci*., 2024, **659**, 463-473.

103 X. Zhou, L. Wu, J. Wang, J. Tang, L. Xi and B. Wang, *J. Power Sources*, 2016, **324**, 33-40.

104 Q. Chen, S. Liu, R. Zhu, D. Wu, H. Fu, J. Zhu and H. He, *J. Power Sources*, 2018, **405**, 61–69.

105 J. Ryu, D. Hong, S. Choi and S. Park, *ACS Nano*, 2016, **10**, 2843–2851.

106 Y.-K. Park, M. Boyer, G. S. Hwang and J.-W. Lee, *J. Electroanal. Chem*., 2019, **833**, 552–559.

107 K. Adpakpang, S. B. Patil, S. M. Oh, J.-H. Kang, M. Lacroix and S.-J. Wang, *Electrochim. Acta*, 2016, **204,** 60–68.

108 X.-Y. Yue, A. Abulikemu, X.-L. Li, Q.-Q. Qiu, F. Wang, X.-J. Wu and Y.-N. Zhou, *J. Power Sources*, 2019, **410-411**, 132–136.

109 L. Sun, T. Su, L. Xu and B. Du, *Phys. Chem. Chem. Phys*., 2016, **18**, 1521–1525.

110 P. Zhang, C. Zhao, W. Ning, S. Miao, L. Nan, Q. Gao and X. Shin, *Colloids Surf. A*, 2022, **642**, 128605-129615.

111 L. Hou, B. Xing, W. Kang, H. Zeng, H. Guo, S. Cheng, G. Huang, C. Cao, Z. Chen and C. Zhang, *Appl. Clay Sci*., 2022, **218**, 106418-106429.

112 X. Huang, D. Cen, R. Wei, H. Fan and Z. Bao, *ACS Appl. Mater. Interfaces*, 2019, **11**, 26854–26862.

113 Y. Lan and D. Chen, *J. Mater. Sci*., 2018, **53**, 2054–2064.

114 D. Alonso-Domínguez, M. P. Pico, I. Álvarez-Serrano and M. L. López, *Nanomaterial*s, 2018, **8**, 805-825.

115 R. A. House, U. Maitra, M. A. Perez-Osorio, J. G. Lozano, L. Jin, J. W. Somerville, L. C. Duda, A. Nag, A. Walters, K.-J. Zhou, M. R. Roberts and P. G. Bruce, *Nature*, 2020, **577**, 502.

116 Y.-E. Huang, W. Lin, C. Shi, L. Li, K. Fan, X.-Y. Huang, X. Wu and K.-Z. Du, *J. Power Sources*, 2021, **494**, 229712.

117 X. Long, Z.-H. Luo, W.-H. Zhou, S.-K. Zhu, Y. Song, H. Li, C.-N. Geng, B. Shi, Z.-Y. Han, G.-M. Zhou, W. Lv and J.-J. Shao, *Energy Storage Materials*, 2022, 52, 120–129.

118 W. Chen, T. Lei, X. Lv, Y. Hu, Y. Yan, Y. Jiao, W. He, Z. Li, C. Yan and J. Xiong, *Adv. Mater*., 2018, **30**, 1804084-1804092.

119 Y. Lan, Y. Liu, J. Li, D. Chen, G. He and I.P. Parkin, *Adv. Sci*., 2021, **8**, 2004036-2004061.

120 F. Wu, H. Lv, S. Chen, S. Lorger, V. Srot, M. Oschatz, P. A. van Aken, X. Wu, J. Maier and Y. Yu, " *Adv. Funct. Mater.,* 2019, **29**, 1902820-1902832.

121 H. Dong, S. Qi, L. Wang, X. Chen, Y. Xiao, Y. Wang, B. Sun, G. Wang and S. Chen, *Small*, 2023, **19** (30).

122 Q. Liu, Y. Zhang, Y. Zhou, M. Wang, R. Li and W. Yue, *J. Solid State Electrochem*., 2023, **27** (3), 797-807.

123 S.-H. Yu, X. Feng, N. Zhang, J. Seo and H. D. Abruna, *Acc. Chem. Res*., 2018, **51** (2), 273-281.

124 B. Jache, J. O. Binder, T. Abe, P. Adelhelm, *Phys. Chem. Chem. Phys.,* 2016, **18** (21), 14299-14316.

125 H. Kim, J. Hong, Y.-U. Park, J. Kim, I. Hwang and K. Kang, *Adv. Funct. Mater.,* 2015, 25 (4), 534-541.

126 Y. Li, Y. Lu, P. Adelhelm, M.-M. Titirici and Y.-S. Hu, *Chem. Soc. Rev*., 2019, **48** (17), 4655-4687.

127 H. Kim, J. Hong and K. Kang, *Energy Environ. Sci.,* 2015, **8** (10), 2963-2969.

128 W. Luo, F. Shen and L. B. Hu, *Acc. Chem. Res.,* 2016, **49** (2), 231-240.

129 J. Sun, H.-W. Lee and Y. Cui, *Nano Lett.,* 2015, **10** (11), 980-U184.

130 Z. L. Jian, W. Luo and X. L. Ji, J. *Am. Chem. Soc*., 2015, **137** (36), 11566-11569.

131 S. Sundaramoorthy, N. Gerasimchuk, K. Ghosh, S.P. Kelley and A. Choudhury, *Chem. Mater*., 2024, **36** (8), 3574-3587.

132 L.S. Zhong, H.N. Chen, W.H. Xie, W.F. Jia, Y.H. Xiao, B.C. Cheng, L.X. Lin and S.J. Lei, *Chem. Eng. J*., 2024, **481**, 148370.

133 R.Z. Wei, Y. Lu, W.J. Ren, Y.P. Han, A.P.V.L. Saroja, X.M. Xia, P. He, C.A.F. Nason, Z.X. Sun, J.A. Darr, J.Y. Luo, M. Zhou and Y. Xu, *J. Phys. Energy*, 2024, **6**, 25022.

134 L. Liu, B.X. Li, J.Q. Wang, H.F. Du, Z.Z. Du and W. Ai, *Small*, 2024, 9647.

135 L.H. Li, S. Lu, X.Y. Wang, J.L. Luo, H. Xu, H.Q, Gu, L. Tan, X. Du, Z.L. Niu, X.C. Zheng and D. Li, *Energy Storage Mater*., 2024, **65**, 103131.

136 W. Ko, S. Lee, H. Par, J. Kang, J. Ahn, Y. Lee, G. Oh, J.K. Yoo, J.Y. Hwang and J. Kim, *Carbon Energy*, 2024, 454.

137 L.P. Duan, C.Y. Shao, J.Y. Liao, L.L. Song, Y.N. Zhang, R.K. Li, S.H. Guo, X.S. Zhou and H.S. Zhou, *Angew. Chem. Inter. Ed*., 2024, **63**(17), 868.

138 Y. Lan, Y. Liu, J. Li, D. Chen, G. He an I.P. Parkin, *Adv. Sci.*, 2021, **8**, 2004036-2004061.

139 X. Cao, S. Yingjuan, Y. Sun, D. Xie, H. Li and M. Liu, *Appl. Clay Sci.,* 2021, **213**, 106265-106273.

140 C. Luo, H. Wang, Y. Qian, X. Shi, Z. Mao, G. Li, C. Yang, Y. Gong, A. Tang and H. Yang, *J. Power Sources*, 2002, **548**, 232038-232047.

141 S. Kajiyama, L. Szabova, K. Sodeyama, H. Iinuma, R. Morita, K. Gotoh, Y. Tateyama, M. Okubo and A. Yamada, *ACS Nano*, 2016, **10** (3), 3334-3341.

142 D. Sabaghi, J. Polcak, H.Y.J. Yang, X.D. Li, A. Morag, D.Q. Li, A.S. Nia, S.H. Khosravi, T. Sikola, X.L. Feng and M.H. Yu, *Adv. Energy Mater*., 2024, **14**(3), 2302961.

143 T. Hosaka, K. Kubota, A. S. Hameed and S. Komaba, *Chem. Rev*., 2020, **120** (14), 6358-6466.

144 M. Song, H. Tan, D. Chao and H. J. Fan, *Adv. Funct. Mater.,* 2018, **28** (41), 1802564.

145 L. Shan, Y. Wang, S. Liang, B. Thang, Y. Yang Z. Wang, N. Lu and J. Zhou, *Infomat*, 2021, 3(9), 1028-1036.

146 A.A. Zhang, X.X. Yin, X. Zhang, J.J. Ba, J.P. Li, Y.J. Wei and Y.Z. Wang, *ACS Appl. Energy Mater*., 2024, **7**(3), 1298-1305.

147 X. Gao, C. Shen, H. Dong, Y.H. Dai, P. Jiang, I.P. Parkin, H.B. Zhang, C.J. Carmalt and G.J. He, *Energy Environ. Sci*., 2024, **17**, 2287-2297.

148 G.F. Shi, P. Zhao, P. Gao, Y.Y. Xing and B.X. Shen, *J. Energy Storage*, 2024, **78**, 110057.

149 Y. M. Li, W. H. Li, W.-Y. Diao, F. Tao, X.-L. Wu and X.-Y. Zhang, ACS Appl. Mater. Interfaces, 2022, **14** (20), 23558–23569.

150 P. Wang, K. Zhang, H. Li, J. Hu and M. Zheng, *Small*, 2023.

151 Q. Liu, P. Zhang, Z. Wang, S. Liu, X. Ren, J. Qian, K. Chen, J. Li, J. Yao and Y. Gan, J. *Alloys Compd*., 2023, **963**.

152 H. Yousefzadeh, A. Noori, M. S. Rahmanifar, N. Hassani, M. Neek-Amal, M. F. El-Kady, A. Vinu, R. B. Kaner and M. F. Mousavi, *Adv. Energy Mater.,* 2023, **13** (41).

153 X. Han, N. Li, J. S. Baik, P. Xiong, Y. Kang, Q. Liu, J. Y. Lee, C. S. Kim and H. S. Park, *Adv. Funct. Mater*., 2023, 33 (11).

154 L. Yang, J. Lu, E. Zhu, J. Zhang, X. Guan, B. Liu, P. Yin and G. Wang, *Appl. Surf. Sci*., 2024, **645.**

155 M. Mao, T. Gao, S. Hou and C. Wang, *Chem. Soc. Rev*., 2018, **47** (23), 8804-8841.

156 S. Kang, K. G. Reeves, T. Koketsu, J. Ma, O. J. Borkiewicz, P. Strasser, A. Ponrouch and D. Dambournet, *ACS Appl. Energy Mater.,* 2020, **3** (9), 9143-9150.

157 F.H. Hsu, S.Y. Hsu, R. Subramani, T.C. Cheng, B.H. Chen, J.L. Chen, J.M. Chen and K.T. Lu, *J. Energy Storage*, 2024, **84A**, 110693.

158 T. Koketsu, J. Ma, B. J. Morgan, M. Body, C. Legein, W. Dachraoui, M. Giannini, A. Demortiere, M. Salanne, F. Dardoize, H. Groult, O. J. Borkiewicz, K. W. Chapman, P. Strasser and D. Dambournet, *Nat. Mater.,* 2017, **16** (11), 1142.

159 S. Heguri, N. Kawade, T. Fujisawa, A. Yamaguchi, A. Sumiyama, K. Tanigaki and M. Kobayashi, *Phys. Rev. Lett*, 2015, **114**(24), 247201/1-247201/5.

160 M. Angell, C.-J. Pan, Y. Rong, C. Yuan, M.-C. Lin, B.J Hwang, and H. Dai, Hongjie. *Proceedings of the National Academy of Sciences of the United States of America*, 2017, **114**(5), 834-839.

161 J. Xu, Y. Dou, Z. Wei, J. Ma, Y. Deng, Y. Li, Yutao, H. Liu, and S. Dou, *Adv. Science*, 2017, **4**(10) 1700146.

162 H. Zhang, Y. Yang, D. Ren, L. Wang, and X. He*, Energy Storage Mater.*, 2021, **36**, 147-170.

163 X. Wu, Y. Chen, Z. Xing, C. Lam, K. Wai, S.-S. Pang, W. Zhang, and Z. Ju, *Adv. Energy Mater.,* 2019, **9**(21), 1900343.

164 Z. Jian, W. Luo and X. *J. Am. Soc.*, 2015, **137**(36), 11566-11569.

165 S. N. Jagadeesan, G. D. Barbosa, F. Guo, L. Zhang, A. M. M. Abeykoon, G. Kwon, D. Olds, C. H. Turner and X. Teng, *Chem. Mater.,* 2023, **35** (16), 6517-6526.

166 Y. Sui, Yiming, C. Li, R.C. Masse, Z. G. Neale, M. Atif, M. AlSalhi and G. Cao, *Energy Storage Mater*, 2020, **25**, 1-32.

167 J. Xu, Jiantie, Y. Dou, Z. Wei, J. Ma, Y. Deng, Y. Li, H. Liu and S. Dou, *Adv. Science,* 2017, **4**(10)

168 S. Xia, X. Wu, Z. Zhang, Y. Cui and W. Liu, *CHEM*, 2019, **5** (4), 753-785.

169 P. G. Balkanloo, A. P. Marjani, F. Zanbili andM. Mahmoudian, *Appl. Clay Sci.,* 2022, **228**, 106632-106644.

170 S. Chua, R. Fang, Z. Sun, M. Wu, Y. Wang, J. N. Hart, N. Shramla, F. Li and D. W. Wang, *Chem.,* 2018, **10** 24(69), 8180-18203.

171 Y. Ma, L. B. Li, L. G. X. Gao, X.-Y. Yang and Y. You, *Electrochim. Acta*, 2016, **187**,535–542.

172 R. Liu, B. Yuan, S. Zhong, J. Liu, L. Dong, Y. Ji, Y. Dong, C. Yang and W. He, Nano Sel.,2021, **2**, 2308–2345.

173 N. Banitaba, D. Semnani, E. Heydari, B. Rezaei and A. A. Ensafi, J. Min. Met. Mater. Soc., 2019, 4537–4546.

144 N.S.M. Johari, S.B.R.S. Adnan and N. Ahmad, *Solid State Ionics*, 2022, **377**, 115882-115891.

175 K. Wissel, S. Dasgupta, A. Benes, R. Schoch, M. Bauer, R. Witte, A. D. Fortes, E. Erdem, J. Rohrer, and O. Clemens*, J. Mater. Chem. A*, 2018, **6**(44), 22013-22026.

176 H. Miki, K. Yamamoto, C. Shuo, T. Matsunaga, M. Kumar, N. Thakur, Y. Sakaguchi, T. Watanabe, H. Iba, H. Kageyama and Y. Uchimoto, *Solid State Ionics*, 2024, **406**, 116480.

177 Q. Yin, T. Wang, Z. Song, S. Yang, Y. Miao, Y. Wu, Y. Sui, J. Qi, Y. Li and D. Zhao, *Chem. Eng. J*., 2023, **459,** 141545.

178 Q. Lin and L. Wang, *J. Semicond*., 2023, 44(4), 041601.

179 Z. Wu, Y. Wu, Q. Yuan, J. Zhang, Y. Dou and J. Han, *ACS Appl. Mater. Interfaces*, 2023, **15**(32), 38540-38549.

180 Z. Song, Q. Yin, S. Yang, Y. Miao, Y. Wu, Y.-Z. Li, Y. Ren, Y. Sui, J. Qi and J. Han, *Small*, 2023, **19**(43), 2302896.

181 D.X. Wang, F.S. Zhang, J.L. Wang, X.Q. Shi, P.L. Gong, H.J. Liu, M.Q. Wu, Y.J. Wei and R.Q. Lian, *J. Mater. Chem. A*, 2024, **12**(14), 8302-8310.

182 Q. Liu, F. Ye, K. Guan, Y. Yang, H. Dong, Y. Wu, Z. Tang and L. Hu, *Adv. Energy Mater*., 2023, **13**, (5), 2202908.

183 S.J. Panchu, K. Raju and H.C. Swart, *Chem. Electro. Chem*., 2024 early access.

184 J. Sarmet, F. Leroux, C. Taviot Gueho, P. Gerlach, C. Douard, T. Brousse, G. Toussaint, P. Stevens, *Molecules*, 2023, **28**, 1006-1020.

185 J. Sarmet, C. Taviot-Gueho, R. Thirouard, F. Leroux, C. Douard, I. Gaalich, T. Brousse, G. Toussaint, and Philippe Stevens, *Cryst. Growth Des*., 2023, **23**(4), 2634-2643.

186 Sarmet, F. Leroux, C. Taviot-Gueho, P. Gerlach, C. Douard, T. Brousse, G. Toussaint, and P. Stevens, *J. Solid State Chem*., 2024, **332**, 124592-124602.

187 Q.Q. Zhang, S.R. Wang, Y.L. Lan, J.P. Deng, M.Z. Fan, G.B. Du and W.G. Zhao, *J. Colloid Inter. Sci.*, 2024, **660**, 597-607.

188 S.S. Cui, X.H. Ren, H.F. Yin, H.Q. Fan, C. Wang, M.C. Zhang, Y. Tang, H.D. Yuan and Y.L. Xin, *J. Energy Storage*, 2024, **85**, 111092.

189 G.A. Muller, J.B. Cook, H.-S. Kim, S.H. Tolbert and B. Dunn, *Nano Lett*., 2015, **15** (3), 1911-1917.

190 P. Xu, H. Xiao, X. Liang, T. Zhang, F. Zhang, C. Liu, B. Lang, and Q. Gao, *Carbon*, 2021,**173**135-144.

191 L. Li, N. Zhang, M. Zhang, X. Zhang, and Z. Zhang, *Dalton Trans*., 2019, 48(5) 1747-1756.

192 Z. Lin, X. Li, H. Zhang, B.B. Xu, P. Wasnik, H. Li, M.V. Singh, Y. Ma, T. Li and Z. Guo, *Inorg. Chem. Front.*, 2023, **10**(15), 4358-4392.

193 X. Wang, S. Kajiyama, H. Iinuma, E. Hosono, S. Oro, I. Moriguchi, M. Okubo and A. Yamada, *Nat. Commun*., 2015, **6**, 6544.

194 L. Zhang, W.-B. Zhang, S.-S. Chai, X.-W. Han, Q. Zhang, X. Bao, Y.W. Guo, X.-L. Zhang, X. Zhou, S.-B. Guo and X.-J. Ma*, J. Electrochem. Soc*., 2021, **168**, 070558.

195 C.H. Chen, Y.Z. Ma and C.L. Wang, *Sustainable Mater. Technol.,* 2019*,* **19**, e00086.

196 S. Maiti, A. Pramanik, S. Chattopadhyay, G. De, and S. Mahanty, J. Colloid Interface Sci.,2016, **464**, 73.

197 Y. Lan, Y. Liu, J. Li, D. Chen, G. He and I. Parkin, *Adv. Sci*., 2021, **8**, 2004036.

198 S. Ummartyoti, N. Bunnak and H. Manuspiya, *Renew. Sust. Energ. Rev*.,2016, **61**, 466–472 View Article Online DOI: 10.1039/D4DT00755G

199 A. Kausar, *Polym. Technol. Eng*.,2017, **57**, 548–564

200 N. Pandi, S.H. Sonawane, A.K. Kola, U.K. Zore, P.H. Borse, S.B. Ambade and M. AshokKumar, *Energy Ecol. Environ.,* 2020, 1–13.

201 C. Cheng, W. Song, Q. Zhao and H. Zhang, *Nanotechnol. Rev*., 2020, **9**(1), 323-344.

202 D. Garcia-Garcia, J. Ferri, L. Ripoll, M. Hidalgo, J. López-Martínez and R. Balart, *Appl. Surf. Sci.*, 2017, **422**, 616-625.

203 W. Xu, B. Mu and A. Wang, *New J. Chem*., 2016, **40**, 2687-2695.

204 N. Y.W. Zaw, S. Jo, J. Park, N. Kitchamsetti, N. Jayababu and D. Kim, *Appl. Clay Sci*.,2022,**225**, 106539-106545.

205 S.S. Chai, L. Zhang, W.-B. Zhang, X. Bao, Y.-W. Guo, X.-W. Han and J. Ma, *Appl. Clay Sci*.,2022, **218,** 106426-106435.

206 J. Zhou, S. Dai, Y. Li, F. Han, Y. Yuan, J. Tang and W. Tang, *Chem. Eng. J*., 2018, **350**, 835–843.

207 J. Jiang, X. Huang, R. Sun, X. Chen and S. Han, *J. Colloid Interface Sci.,* 2023, **640**,662-679.

208 Y. Zhao, Y. Li, X. Quan and C. Li, *Electrochim. Acta*, 2019, **321**, 134715.

209 R. Baby Suneetha, *ECS Trans.,* 2022, **107**(1), 4003.

210 S. Zhang, Y. Yang, R. Xiao, M. Yu, Y. Zhang, X. Sun, L. Lu, X. Wu and Y. Chen, *Appl. Clay Sci*., 2021, **200**, 105821-105830.

211 G. Chen, Y. Ai, I.T. Mugaanin, W. Ma, B.S. Hsiao, K. Hoi and M. Zhu, *J. Power Sources*,2020, **450**, 227637-227676.

212 R. Oraon, A. De Adhikari, S.K. Tiwari and G.C. Naya, *Dalton Trans.,* 2016, **45**, 9113-9126.

213 M. Ates and S. Caliskan, *Polym.-Plast. Technol. Mater*., 2019, **58**(14), 1481-1494

214 W. Ge, Q. Ma, Z. Ai, W. Wang, F. Jia and S. Song, *Appl. Clay Sci.,*2021, **206**, 106022-106030

215 X. Yang, X. Zeng, G. Han, D. Sui, X. Song and Y. Zhang, *Nanomaterials*, 2020, **10**, 1703-1720.

216 S. Guo, K. Zhao, Z. Feng, Y. Hou, H. Li, J. Zhao, Y. Tian and H. Song, *Appl. Surf. Sci.,* 2018, **455**, 599–607.

217 C. Wu, T. Zhou, Y. Du, S. Dou, H. Zhang, L. Jiang and Q. Cheng, *Nano Energy*, 2019, **58**, 517–527.

218 A.B. Ganganboinaa, A. Dutta Chowdhury and R. Doong, *Electrochim. Acta*, 2017, **245**, 912–923.

219 S.K. Shinde, D.P. Dubal, H.M. Yadav, A.D. Jagadale, N. Maile, S.S. Karade, D.-S. Lee, and D.-Yo. Kim, *Ceram. Int*.,2022, **48**, 25020–25033.

220 S.S. Chai, W.-B. Zhang, J.L. Yang, L. Zhang, X.-W. Han, M.M. Theint and X.-J. Ma, *J. Rare Earths*, 2023, **41**, 728–739.

221 S. Venkatesan and Y.-L. Lee, *Coord. Chem. Rev*., 2017, **353**, 58–112.

222 H. Iftikhar, G.G. Sonai, S.G. Hashmi, A.F. Nogueira and P.D. Lund, *Materials*, 2019, **12**, 1998–2066.

223 S. Ummartyoti, N. Bunnak and H. Manuspiya, *Renew. Sust. Energ. Rev*., 2016, **61**, 466–472.

224 Y. Li, J.V. Milic, A. Ummadisingu, J.Y. Seo, J.H. Im, H.S. Kim, Y. Liu, M.I. Dar, S.M. Zakeeruddin, P. Wang, A. Hagfeldt and M. Grätzel, *Nano Lett*., 2019, **19**(1), 150-157.

225 F. Long, Y.H. Guo, L.G. Yuan, H. Yin, Y.R. Tao, Z.G. Jiang, S.M. Peng, B. Wu, K.Y. Yan, M. Liu, X.H. Lu, W.W. Meng, M.Z. Long and G.F. Zhou, *Chem. Eng. J*., 2024, **485**, 149963.

226 S. Yun, J.N. Freitas, A.F. Nogueira, Y. Wang, S. Ahmad and Z.-S. Wang, *Prog. Polym. Sci*., 2016, **59**, 1–40.

227 D. Costenaro, C. Bisio, F. Carniato, G. Gatti, F. Oswald, T.B. Meyer and L. Marchese, *Sol. Energy Mater. Sol. Cells*, 2013, **117**, 9–14.

228 R.K. Gupta, H.-W. Rhee, I. Bedja, A.N. AlHazaa and A. Khan, *J. Power Sources*, 2021, **490**, 229509.

229 C.W. Tu, K.Y. Liu, A.T. Chien, M.H. Yen, T.H. Weng, K.C. Ho and K.F. Lin, *J. Polym. Sci., Part A :Polym. Chem.*, 2008, **46**, 47–53.

230 M.A.S. Andrade, A.F. Nogueira, K. Miettunen, A. Tiihonen, P.D. Lund and H.O. Pastore, *J. Power Sources*, 2016, **325**, 161–170.

231 L.-H. Chen, S. Venkatesan, I-P. Liu and Y.L. Lee, *J. Oleo Sci,* 2020, **69**(6), 539-547.

232 N. Sangiorgi, A. Sangiorgi, A. Sanson, M. Licchelli, M. Orbelli, and A. Biroli, *Processes*, 2023, **11**, 463-475.

233 Z. Chen, K. O. Kirlikovali, K. B. Idrees, M. C. Wasson and K. Farha, *Chem*, 2022, 8, 693–716,

234 S. Flesch, D. Pudlo, D. Albrecht, A. Jacob and F. Enzmann, *Int J Hydrogen Energy*, 2018, **43**, 20822-20835.

235 C. Hemme and W. Van Berk, *Appl Sci*., 2018, **8**, 2282.

236 A. Al-Yaseri, D. Wolff-Boenisch, C.A. Fauziah, and S. Iglauern, *Int J Hydrogen Energy,* 2021, **46**, 34356-34361. DOI: 10.1039/D4DT00755G View Article Online

237 P. Ghosh, B. Kumar Prusty, P. Sandilya and V. Y. Turlapati, *Energy Fuels*, 2023, 37, 6757−6769.

238 V. A. Arus, S. Nousir, E. Sennour, T. C. Shiao, I. D. Nistor, R. Roy and A. Azzouz, *Int J Hydrogen Energy*, 2018, **43**, 7964-7972.

239 Alver, B. E. *Clay Miner.,* 2017, **52** (1), 67−73.

240 A. Azzouz, S. Nousir, N. Bouazizi and R. Roy, *TechConnect Briefs*,2014, **3**, Nanotechnology 2014: Electronics, Manufacturing, Environment, Energy & Water, 489 – 492.

241 R. Sennour, T. C. Shiao, V. A. Arus, M. Nazir Tahir, N. Bouazizi, R. Roy and A. Azzouz, *Phys. Chem. Chem. Phys.*, 2017, **19**, 29333-29343.

242 Samimi, M. Ghiyasiyan-Arani and M. Salavati-Niasari, **Fuel**, 2022, **320**, 123933-123945.

243 R. Naresh Muthu, S. Rajashabala and R. Kannan, *Renewable Energy*, 2016, **90**, 554-564.

244 R. Monsef and M. Salavati-Niasari, *Fuel*, 2023, **332**, 126015-126031.

245 J. S. Boruah and D. Chowdhury, *Minerals*, 2023, **13**, 26.

246 C. Ruiz-García, J. Pérez-Carvajal, A. Berenguer-Murcia, M. Darder, P. Aranda and E. Ruiz-Hitzky, *J. Phys. Chem. Chem. Phys*., 2013, **15**, 18635-18641.

247 L. Daukiya, M. N. Nair, M. Cranney, F. Vonau, S. Hajjar-Garreau, D. Aubel and L. Simon, *Prog. Surf. Sci.,* 2019, **94**(1), 1-20.

248 T. E. Weller, M. Ellerby, S. S. Saxena, R. P. Smith and N. T. Skipper, *Nature Phys*., 2005, **1**, 39**.,** C. Emery, M. Hérold, V. d'Astuto, Ch. Garcia, J.-F. Bellin, J, Marêché, P. Lagrange and G. Loupias*, Phys. Rev. Lett*., 2005,19; **95**(8):087003.

249 I. El Hajj, L. Speyer, S. Cahen, L. Herbuvaux, P. Lagrange, G. Medjahdi and C. Herold, *Carbon*, 2022, **186**, 431-436.

250 S. Ichinokura, K. Sugawara, A. Takayama, T. Takahashi and S. Hasegawa*, ACS Nano*, 2016, **10** (2), 2761-2765.

251 M. Yankowitz, S. Chen, H. Polshyn, Y. Zhang, K. Watanabe, T. Taniguchi, D. Graf, A. F. Young and C. R. Dean, *Science*, 2019, **363**(6431), 1059-1064.

252 M. A. Choffel, R. N. Gannon, F. Goehler, A. M. Miller, D. L. Medlin, T. Seyller and D. Johnson, *Chem. Mater.,* 2021, **33** (16), 6403-6411.

253 K. Nakayama, H. Kimizuka, Y. Tanaka, T. Sato, S. Souma, T. Takahashi, S. Sasaki, K. Segawa and Y. Ando, *Phys. Rev. B*, 2015, **92** (10), 100508- 100513.

View Article Online
DOI: 10.1039/D4DT00755G

254 S. Paul, B. Dalal, R. Jana, A. Shit, A. Datta and S. Kumar De, *J. Phys. Chem. C*, 2020, **124**(23), 12824-12833.

255 B. Soundiraraju and B.K. George, *ACS Nano*, 2017, **11**(9), 8892-8900.

256 J.L. Andrews, L.R. De Jesus, T.M. Tolhurst, P.M. Marley, A. Moewes and S. Banerjee, *Chem. Mater*., 2017, **29**(7), 3285-3294.

257 J.P. Pender, G. Jha and C.B. Mullins, *ACS Nano*, 2020, **14**(2), 1243-1295.

258 T. Liu, L. Lin, X. Bi, L. Tian, K. Yang, J. Liu, M. Li, Z. Chen, J. Lu, M. Li, Z. Chen, J. Lu, K. Amine, K.Xu, F. Pan, *Nat. Nanotechnol.*, 2019, **14**(1), 50-56.

259 H. Kim, J. Hong and K. Kang, *Energy Environ. Sci*., 2015, **8**(10), 2963-2969.

260 X. Bie, K. Kubota, T. Hosaka, K. Chihara, and S. Komaba, *J. Mater. Chem. A*, 2017, **5**(9), 4325-4330.

261 L. Fan, R. Ma, Q. Zhang, X. Jia, B. Lu, *Angew. Chem. Int. Ed*., 2019, **58**(31), 10500-10505.

262 Y. Ishijima, H. Imai and Y. Oaki, *Chem.,* **3**(3), 509-521.

263 A. Rouag, R. Porhiel, K. Lemoine, F. Leroux, J.M. Grenèche, D. Delbègue, C. Iojoiu, K. Guérin, *Dalton Trans*., 2024, **53**(17), 7628.

264 D.D. Zhu, Y. Su, J.Z. Chen, X.Z. Ou, X.D. Zhang, W. Xie, Y.Y. Zhou, Y.N. Guo, Q.S. Dai, P. Jia, J.T. Yan, L. Geng, B.Y. Guo, L.Q. Zhang, Y.F. Tang, Q. Huang and J.Y. Huang, *Nanoresearch*, 2023, 6289.

265 S.W. Liu, J.C. Yang, S.P. Hao, S.J. Jiang, X.H. Li, O. Dolotko, F.X. Wu, Y.J. Li and Z.J. He, *Chem. Eng. J*., 2024, **479**, 147607.

266 Ghosh, M. Bhar, U. Bhattacharjee, K.P. Yalamanchili, S. Krishnamurthy and S. K. Martha, *J. Mater. Chem. A*, 2024, **12**, 11362-11377.

267 G. Liu, L. Ma, X. Xi, Z. Nie, *Waste Management*, 2024, **178(15)**, 105-114

268 Y. Gao, S. Zhang, S. Lin, Z. Li, Y. Chen, C. Wang, *Environmental Research*, 2024, **247**, 118216.

269 S. Yang, Q. Gao, Y. Li, H. Cai, X. Li, G. Sun, S. Zhuang, Y. Tong, H. Luo, M. Lu, *J. Energy Climate*, 2024, **93**, 24-31

270 M.G. Kanatzidis, L.M. Tonge, T.J. Marks, H.O. Marcy, and C.R. Kannewurf, J. Am. Chem. Soc., 1987, 109, 12, 3797-3799.

271 P. Vialat, C. Mousty, C. Taviot-Gueho, G. Renaudin, H. Martinez, J.-C. Dupin, E. Elkaim, and F. Leroux, *Adv. Funct. Mater*., 2014, **24**, 4831-4842.